MDAG.com Internet Case Study 71

The Complex Three-Phase Effects of Humidity on Small-Scale Water Films and Reactive Mineral Surfaces

by K.A. Morin
© 2021 Kevin A. Morin
www.mdag.com/case_studies.html

Abstract

The main objective of this MDAG Case Study is to understand better the interactions between various phases of H_2O relevant to minesite components and to other open environmental systems containing combinations of minerals. These H_2O phases, as they can occur within minesite components, are: (gaseous) vapour expressed as humidity, liquid water particularly in microscopic water films, and solid H_2O in "hydrated" minerals with waters-of-crystallization.

Based on a literature review and the re-interpretation of some information, the interactions and the positive and negative feedback loops among the H_2O phases are numerous and complex (summarized in Figure 7-1). These are not easily understood intuitively or modelled.

For the vapour phase, relative humidity (RH) was found to be more important for understanding the interactions than absolute humidity (AH). This is because RH is related to the linked H_2O chemical activities in the vapour and water. The interactions among RH and the other H_2O phases are complex (summarized in Figure 7-2).

Table of Contents

List of Tables

List of Figures

1. Introduction

Special Note: This MDAG Case Study is based on air as the primary gas phase, close to 101.3 kPa (1 standard atmosphere). Mixtures of other gases and at other pressures may lead to significant deviations not discussed below.

This MDAG Case Study contains a literature review and the re-interpretation of that literature. The main objective is to understand better the interactions between various phases of H_2O relevant to minesite components and to other open environmental systems containing combinations of minerals. This work is driven by the recent studies of Dy et al. (2021) and Ma et al. (2019 and submitted).

H_2O can occur in three phases in and around minesite components: vapour (humidity), liquid (water), and solid (Figure 1-1). In this Case Study, rather than ice (frozen water), the solid form of primary interest is in "hydrated" minerals as part of waters-of-hydration in crystal structures (e.g., $CaSO_4 \bullet 2H_2O$) and in amorphous compounds as bound water molecules (e.g., amorphous $Fe(OH)_3$). Physically, the dividing lines among these phases and forms of H_2O can sometimes be ambiguous and uncertain. For example, liquid water and solid-phase minerals combined as one "water film" can occur as a gel or amorphous quasi-solid like hydrous ferric oxyhydroxides, instead of two distinct phases.

It turns out that this necessitates dividing minerals into two endpoints: (1) "relatively insoluble" with a simplified "hard surface" on crystal faces and (2) "relatively soluble" with a "soft surface" somewhere between solid and liquid. In some ways, this is synonymous with the division into hygroscopic and deliquescent minerals, but this division does not adequately allow for some of the observations discussed in this Case Study. Between these two endpoints are other minerals, such as hydrated minerals like gypsum. This is explained in more detail in the following sections.

It appears to be widely acknowledged that minerals surfaces exposed to natural environmental and climatic conditions will be coated with thin, often microscopic, "water films". For example, Santos and Verdaguer (2016) wrote,

> *"All surfaces exposed to ambient conditions are covered by a thin film of water. Other than at high humidity conditions, i.e., relative humidity higher than 80%, those water films have nanoscale thickness. Nevertheless, even the thinnest film can profoundly affect the physical and chemical properties of the substrate."*

Boily et al. (2015) added,

> *"Atmospheric water vapor interacts with all solid surfaces present in nature, including minerals, bacteria and plants."*

Minesite components contain rock surfaces and particles with various minerals exposed to natural environmental and climatic conditions. Thus, these surfaces and particles typically contain water films, even when they are only of microscopic thicknesses and not readily detectable such as through "moisture content". Also, simplistic scenarios indicating no water films exist due to evaporation at low relative humidity (RH), like 15% RH, can be incorrect, as explained in detail in this Case Study.

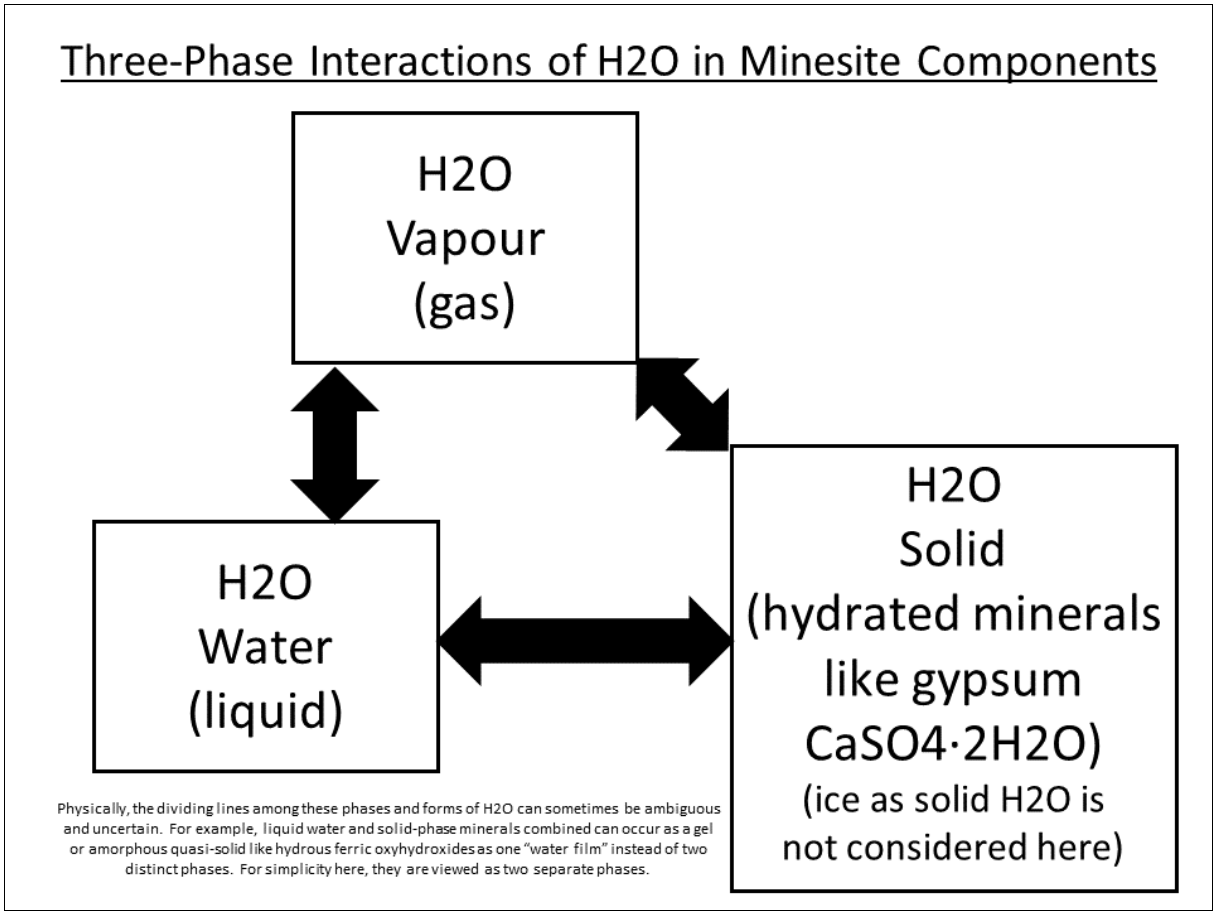

Figure 1-1. The three phases of H_2O considered here for minesite components, with solid H_2O limited here to minerals containing waters of hydration; the division into these three phases is not always distinct such as with gels and quasi-solids forming water films on mineral surfaces.

Therefore, water films on mineral surfaces should be expected in virtually all minesite components around the world and thus are important for understanding and predicting mineral reactivities and water chemistries (e.g., Ma et al., 2019 and submitted). However, the properties of these water films can vary significantly in three spatial dimensions and can display dynamic behaviours through time.

A major part of these spatial and temporal variabilities is caused by the three-phase interactions of humidity (vapour), water, and solid-phase H_2O, made more complex by relative phase mobility and immobility and by variable solubilities.

Mobilities for the three phases of H_2O can be generally summarized as follows.

- Solid H_2O in minerals and amorphous compounds can often be considered immobile. This is because minerals and compounds containing H_2O have limited mobility in minesite components. Nevertheless, they can move as the rock particles weather, break apart, compact, settle, and sometimes travel with infiltrating water.

- Microscopic water films are often considered immobile because of physical and chemical forces that bind portions of these small-scale films to mineral surfaces (e.g., Yeşilbaş and Boily, 2016). Locally, there can be an exchange of the immobile solid H_2O from within minerals to the immobile aqueous water-film H_2O or to the mobile vapour (discussed in Section 5 below). Macroscopically, water films located on active water flowpaths can be at least partially flushed and replaced by flowing water.

- Humidity is part of the air phase, and thus can be mobile under gradients such as barometric, temperature, and pressure. Total gas pressures within minesite components are typically close to one atmosphere, but can vary spatially and temporally due to external winds, gas consumption by water and solid minerals, etc. Thus, the gas phase and its humidity in minesite components are considered mostly mobile in this Case Study. Gas-phase mobility in minesite components is often incorrectly considered negligible and reflecting extremely slow diffusion, but there are reasons why this mobility is typically higher (Morin, 2021).

At this point, it is helpful to clarify some details on absolute and relative humidities.

2. Absolute and Relative Humidity

There are various types of defined "humidities", with the focus here on absolute humidity (AH) and relative humidity (RH). As shown in this Case Study, these relatively simple concepts for the air phase can lead to impressively complex situations with associated aqueous and solids phases.

Absolute humidity is defined as the mass of water vapour divided by the volume of the air phase including the water vapour (e.g., Wikipedia, 2021a):

Absolute Humidity (AH) = Mass of H_2O vapour / Total volume of air and H_2O (Eq. 2-1)

Although this Case Study is focussed on air, it is interesting to note that Equation 2-1 still applies when "air" is replaced by "vacuum". This is because the partial pressure of water vapour is ideally, but not exactly, independent of the presence of other gases and their partial pressures (Bonanno et al., 1994).

Relative humidity is not based on the mass of water vapour like Absolute Humidity, but instead on the partial pressure of the water vapour (e.g., Wikipedia, 2021a):

Relative Humidity (RH) = Partial pressure of H_2O vapour /
Equilibrium (maximum) pressure of H_2O vapour over a flat surface of pure water (Eq. 2-2)

Here are some important points hidden in Equations 2-1 and 2-2.

- Maximum AH (theoretically occurring at 100% RH) is temperature dependent (Figure 2-1), with maximum AH increasing substantially as temperature increases (e.g., Stull, 2017). For example, the maximum mass of water vapour and its partial pressure are roughly 10 times higher at 50°C than at 10°C. In this range, one m^3 of air can contain roughly 10 to 100 grams of H_2O.
- RH is based on pressure (e.g., kPa) rather than mass/volume like AH (e.g., g/m^3), but the two are correlated (Figure 2-1 based on RH=100%). The relationship based on temperature in Kelvin is (Stull, 2017):

  AH (g/m^3) = 2170 * Partial pressure of water vapour (kPa) / [T (in K)] (Eq. 2-3)
- The denominator of Equation 2-2 is the maximum pressure of water vapour "over a flat surface of pure water". These words are critical, because water films on natural mineral surfaces are not pure water and can even become concentrated brines. As explained in Section 3 below, this means that an equilibrated RH of 100% cannot be easily maintained in air over natural water films, which carries important implications for mineral reactivity. Also, mineral surfaces are not necessarily flat (implying the application of some uncommon version of the Kelvin Equation), but this effect is not discussed here as it is relatively unimportant.

Because the maximum mass of water vapour and its partial pressure are roughly 10 times higher at 50°C than at 10°C as an example, one might think that AH is more important for water films and mineral reactions than RH. However, it is not that simple.

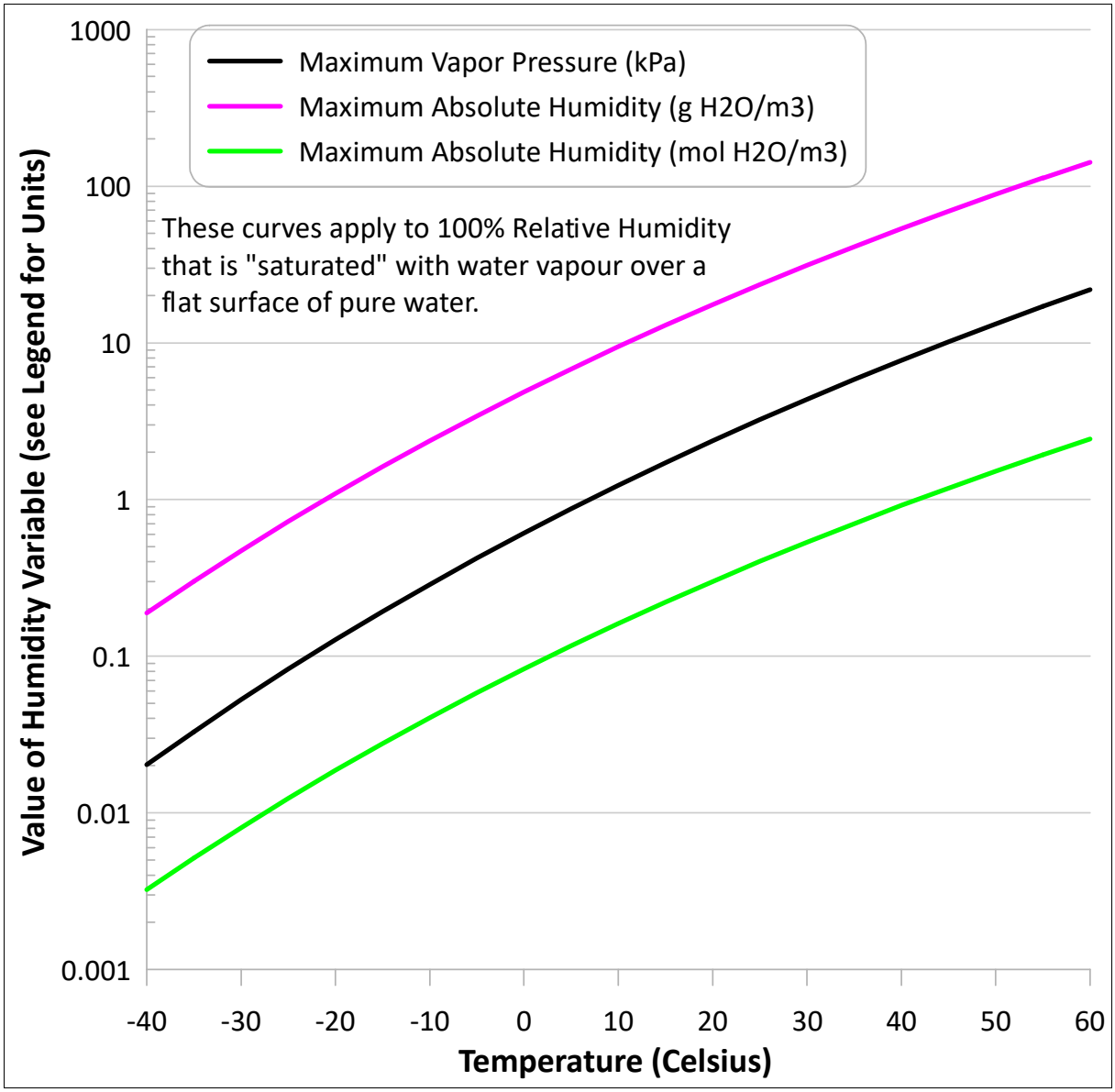

Figure 2-1. The maximum "equilibrium" values for water-vapour pressure and unit-volume mass in the air phase as temperature changes (from data in Stull, 2017).

! " # $%& '(
) * (* +

,
-! % . . ! % . . - ! * % !' & /%
0 " . 123/ . $3 0 ! % -! % . " / . / . !' & 2%
4 * *) *&

+) 5 6 7 ! 88/% * (!' 2% + +
* + + ! 0 9%
:) * ;2< !
6 % + .
* & 4) +
* *
& & &) * !$8<%) (6
*) * &=
(" * + *
+ 7 & 4 + * * !' 2% *
( )) 7 + (" *&

>) * * *
7 ! ' 7) * (" -%& * *
7 !" 2%& 4 7) * +
) +) * + + ! '
" -&1 +%&) * + +
7 & +
! & & ' / 2% 7 !0 1%&

> ((* * (
7 & 4 ? (? *
" * : (4 ' * & & & = + + +
" & 0 (7
* * &

> * ( ) *
* ' / *,
. ! % . . - 8 . . . . - . . -! % . . !' & #%

+)) + * * *
' # +) + + $
- + & 4)
) * + * " -&

3. Equilibrium Relative Humidity (ERH) and Relatively Soluble Minerals

3.1 Concepts and Explanations

A common simplification is that liquid water will evaporate into stagnant air below 100% relative humidity (RH) to raise RH towards 100% and eventually reach 100% if sufficient water is present. While generally true of pure water and tap water in closed or in mildly dynamic systems, it is not true of water when it contains substantial amounts of dissolved ions. "Substantial amounts" in this case means "relatively soluble" minerals and compounds like NaCl and KCl encountered during mining for halite and potash and like some sulphate minerals.

The "preferred" and "stable" relative humidity of a saturated aqueous solution containing excess hygroscopic soluble solid-phase salt in a closed, equilibrated system is called the Equilibrium Relative Humidity (Wikipedia, 2021b). ERH can be defined on an empirical basis as the relative humidity at a particular temperature at which a solid soluble hygroscopic material neither gains nor loses moisture (note: this definition involves solid and liquid phases). Based on simplifications of Raoult's Law and Henry's Law, ERH can be defined mathematically (note: this involves the liquid phase) as:

$$\text{Equilibrium Relative Humidity (ERH)} = a_{water} * 100\% \quad \text{(Eq. 3-1)}$$

and

$$a_{water} \sim l_{water} * x_{water} \quad \text{(Eq. 3-2)}$$

where a_{water} = chemical activity of water in an aqueous solution
l_{water} = chemical activity coefficient of water in an aqueous solution
x_{water} = mole fraction of water in an aqueous solution

In pure water, $l_{water} = 1.0$ and $x_{water} = 1.0$, so ERH = 100%. Tap water typically has relatively low aqueous concentrations and thus its ERH is slightly less than 100%.

A simplistic and not highly accurate equation for calculating RH in equilibrium with aqueous concentrations in water, from undersaturation up to saturation (from 100% RH down to ERH), is:

$$RH = 100 * a_{water} = 100 * M_{water} / (M_{water} + N * M_{mineral}) \quad \text{(Eq. 3-3)}$$

where M_{water} = molar mass of water in solution (moles of H_2O/L of total solution)
$M_{mineral}$ = molar mass of soluble mineral in solution (moles of mineral/L of total solution)
N = number of ionic components from a soluble mineral (e.g., N=2 for NaCl and LiCl) assuming full dissociation in solution which is rarely the case

For NaCl with an atomic mass of 58.44 and H_2O with an atomic mass of 18.02, 1 L of fully saturated solution at 20°C contains 359.2 g NaCl/L (6.146 M NaCl) with a solution density of 1.2 kg/L and an ERH of 75% (Olynyk and Gordon, 1943). The ideal results of Equation 3-3 are plotted against measured RH for NaCl in Figure 3-1, showing greater discrepancies as NaCl increases towards saturation. For more than one soluble mineral dissolved in water, a complex "additive rule" based on ionic strength and per-mole contributions of the minerals applies (Robinson and Bower, 1965a and 1965b).

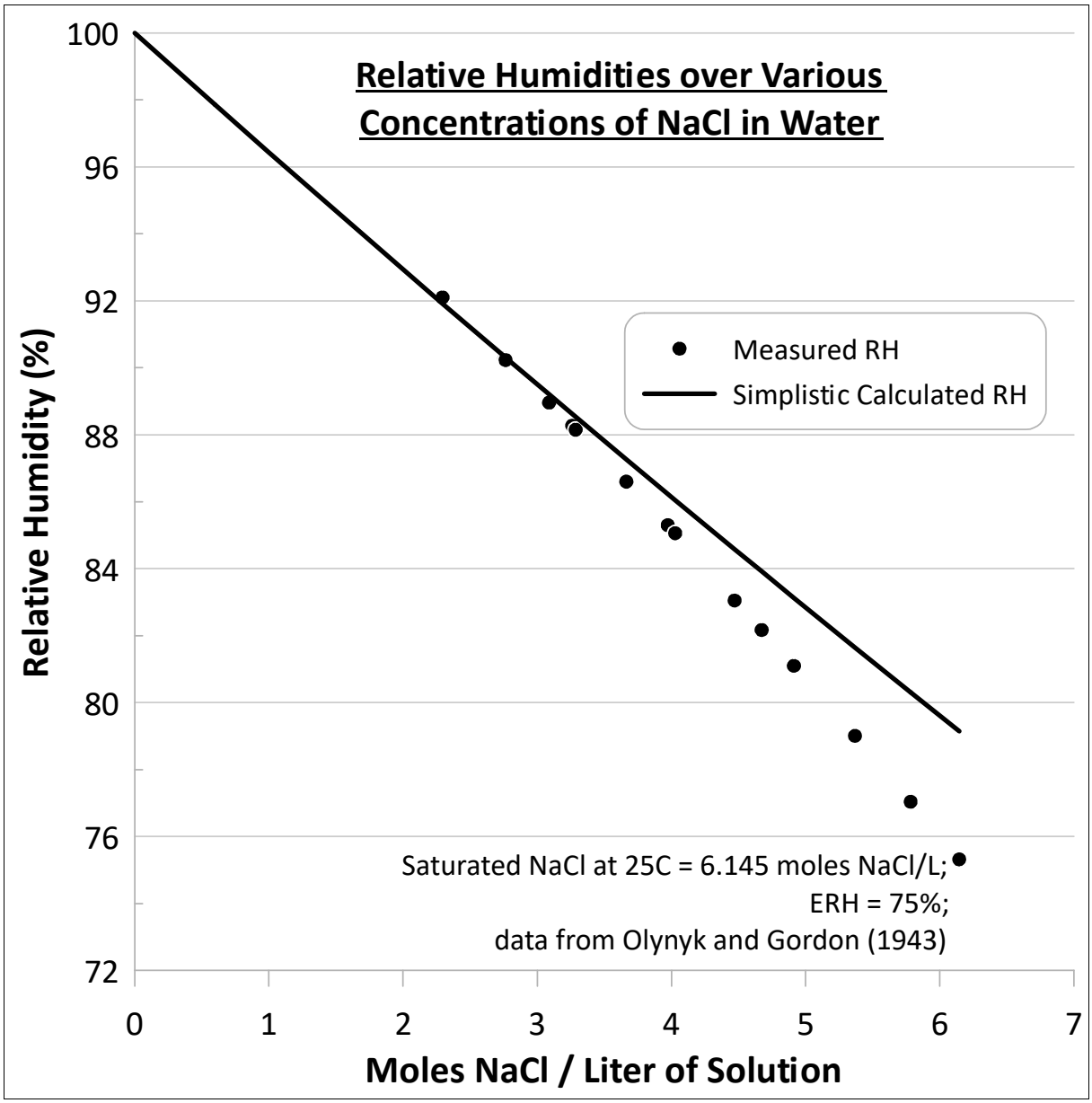

Figure 3-1. Relative humidity (RH) over aqueous solutions with various concentrations of NaCl with calculated RH from Equation 3-3 and measured data from Olynyk and Gordon (1943).

Interestingly, seawater contains about 35 parts per thousand of dissolved ions, mostly Na^+ and Cl^-. This is equivalent to approximately 0.6M NaCl/L in Figure 3-1with an RH of approximately 98%. Anomalously, ocean-water RH is around 80% (e.g., Geophysical Fluid Dynamics Laboratory, 2014), which seems a contradiction. However, RH above the oceans varies spatially and temporally due to factors like dynamic movements of ocean waters and overlying air, temperature variations, height of measurement above the air-ocean contact (e.g., 2 m), etc.

Returning to fully saturated solutions of relatively soluble minerals, Table 3-1 (from Greenspan, 1977) lists some ERH values and Figure 3-2 shows trends of some ERH values with changing temperature. Dozens of additional ERH values can be found in references like O'Brien (1948), Wexler and Hasegawa (1954), and Winston and Bates (1960), but it is important to note that the concept of ERH is more complex with pairs of hydrated minerals (Section 5). Carotenuto and Dell'Isola (1996) argued that values like those in Table 3-1 have errors due to older measurement techniques and to not waiting at least 12 hours for stabilization, but the errors are typically relatively small.

Cycling between 20% and 98% RH (above and below ERH values) every six hours at 20°C with no liquid water can lead to flaking, slaking, and breaking of rocks like tuffs and sandstones (Sato and Hattanji, 2018). In turn, this can accelerate the bulk chemical reactivity due to newly exposed minerals. The degree of breaking correlated with a mineral's ERH, with the lowest ERH (NaCl) producing the greatest breakage within 100 cycles.

Richardson and Malthus (1955) focussed on compounds with lower values of ERH and listed ERH values at 25°C for dozens of inorganic compounds (and more organic compounds) in groups from 0-10% RH to 50-60% RH. Their Table II (partially reproduced here in Table 3-2) showed how ERH values at 25°C varied with the cationic and anionic element.

In minesite components, each soluble mineral can create different aqueous concentrations when dissolved to saturation and equilibrium. As a result, each can have and create a unique ERH value at saturation, which some have called "humidity buffers" since they can maintain a relatively constant RH value (discussed below for Figures 3-3 and 3-4). Below equilibrium and saturation, equilibrated RH values will lie between the saturation-based ERH and 100% RH. In reality, mixtures of saturated solutions caused by combinations of minerals dissolving to equilibrium will create a single composite ERH rather than individual ERH values when well mixed and combined.

As an alternative to soluble natural minerals, cement paste has an ERH of approximately 80% (e.g., Flatt and Bullard, 2011). However, this ERH can vary significantly with added binders and compounds (e.g., Zhang et al., 2019).

An aqueous concept similar to ERH in the gas phase is "equilibrium moisture content" (EMC) in a wet solid phase (Wikipedia, 2021c):

> "The equilibrium moisture content (EMC) of a hygroscopic material surrounded at least partially by air is the moisture content at which the material is neither gaining nor losing moisture. The value of the EMC depends on the material and the relative humidity and temperature of the air with which it is in contact."

Table 3-1. Examples of Equilibrium Relative Humidity (ERH in %) over solutions saturated with excess soluble mineral at 25°C (from Greenspan, 1977)

Lithium Bromide	6.37	Lithium Chloride	11.30
Lithium Iodide	17.56	Potassium Fluoride	30.85
Magnesium Chloride	32.78	Potassium Carbonate	43.16
Magnesium Nitrate	52.89	Cobalt Chloride	64.92
Strontium Chloride	70.75	Sodium Nitrate	74.25
Sodium Chloride	75.29	Ammonium Chloride	78.57
Ammonium Sulphate	80.99	Potassium Chloride	84.34
Strontium Nitrate	85.06	Potassium Nitrate	93.58
Potassium Sulphate	97.30	Potassium Chromate	97.88

Table 3-2. Examples of Equilibrium Relative Humidity (ERH in %) over solutions saturated with various combinations of cations and anions at 25°C (from Richardson and Malthus, 1955)

	Chloride	Thiocyanate	Permanganate	Nitrate
Lithium	11.1	12.5		47.1
Sodium	75.3	35.7	61.6	73.8
Potassium	84.3	46.6		92.5
Magnesium	32.4	47.7		52.9
Zinc	<7	80.4	51.2	~38
Calcium	28.85	17.6	37.4	50.5
Strontium	70.8	31.9		
Barium	90.2	54.7		

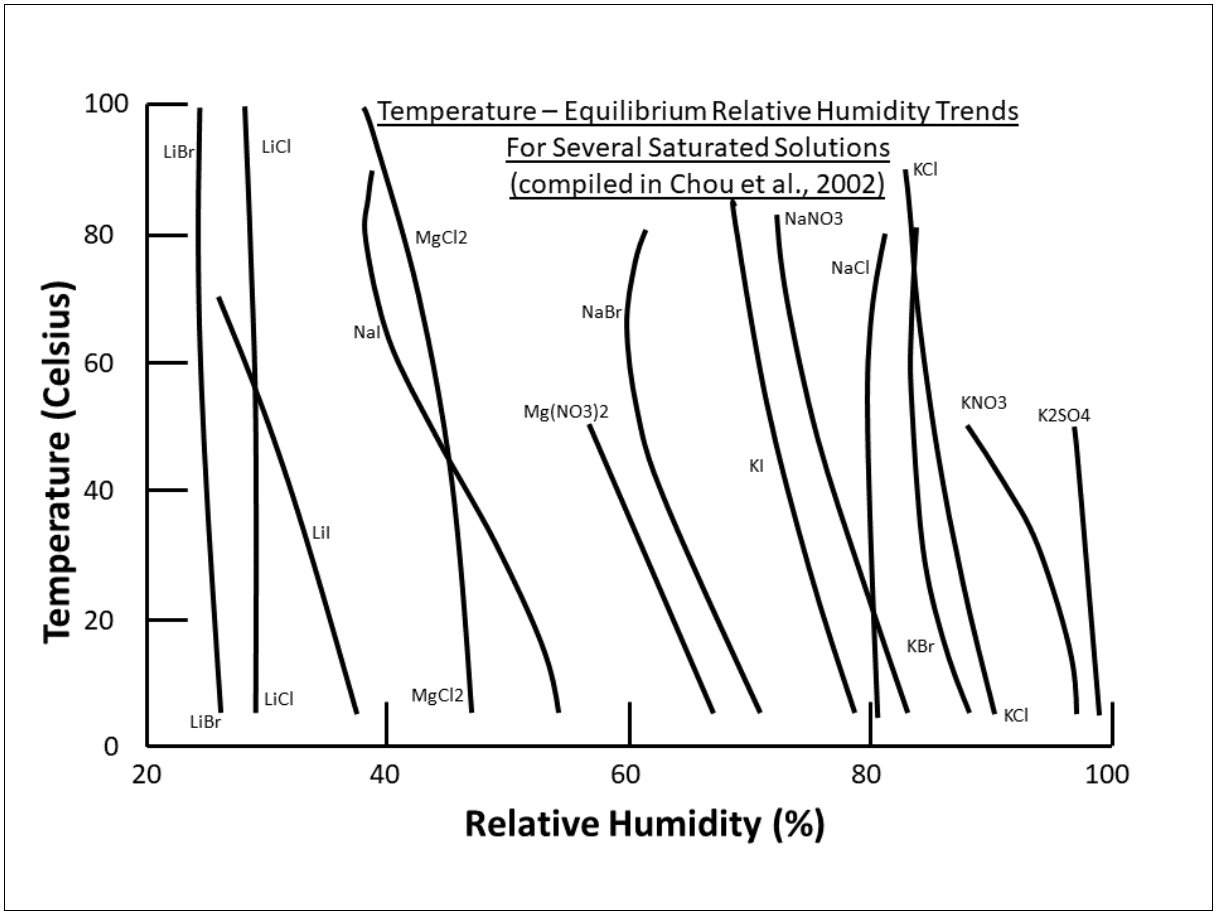

Figure 3-2. Trends in Equilibrium Relative Humidity with changing temperature for selected relatively soluble minerals (compiled in Chou et al., 2002).

> "The speed with which [the EMC] is approached depends on the properties of the material, the surface-area-to-volume ratio of its shape, and the speed with which humidity is carried away or towards the material (e.g. diffusion in stagnant air or convection in moving air)."

Theoretically, the EMC of the combined solid and water is attained when the ERH is maintained in the air so that there is no gain or loss of H_2O in any of the three phases. At constant RH, the EMC will reportedly decrease by roughly 0.5% with an increase of 10°C in air temperature.

Based on the preceding discussion, some interesting observations on H_2O phases can be derived from considering the movement of air over:

- a single salt-saturated solution (Figure 3-3 for soluble NaCl), and
- two salt-saturated solutions (Figure 3-4 for soluble NaCl and LiCl), with LiCl having a much lower ERH according to Equation 3-3 and Table 3-1 due to its much higher solubility in water.

For example:

- Given enough time and a relatively constant temperature, air at 100% RH passing over a NaCl-saturated solution with excess solid NaCl in a "bucket" will have its RH reduced to ~75%, while water is continuously added to the bucket by the extracted humidity (top of Figure 3-3).

- Given enough time and a relatively constant temperature, air at 30% RH passing over a NaCl-saturated solution with excess solid NaCl in a "bucket" will have its RH increased to ~75%, while water is continuously removed from the bucket to raise the RH (bottom of Figure 3-3).

- Given enough time and a relatively constant temperature, air at 20% RH passing over both a NaCl-saturated solution with excess solid NaCl in one "bucket" and a LiCl-saturated solution with excess solid LiCl in another bucket will have its net RH reduced to ~11%. The NaCl solution attempts to raise RH to 75% (for as long as it contains H_2O), but the LiCl solution removes humidity down to ~11% (Figure 3-4). Note: this example is one simplified analogue for why minerals inside minesite components can retain some geochemical reactivity under arid conditions or seasonally dry conditions with low RH values, in addition to any physical condensation under daily and seasonal temperature variations.

- At the point when H_2O is depleted from a bucket by releasing all H_2O to humidity, leaving only solids, then the effects of that bucket on the RH and the other phases of H_2O cease. On the other hand, at the point when excess solid salt is fully dissolved from a bucket by reducing humidity, then the effects of that bucket on the RH and the phases of H_2O decrease with time as the activity of water (Equation 3-1) increases. Note the hysteresis created by these opposing trends.

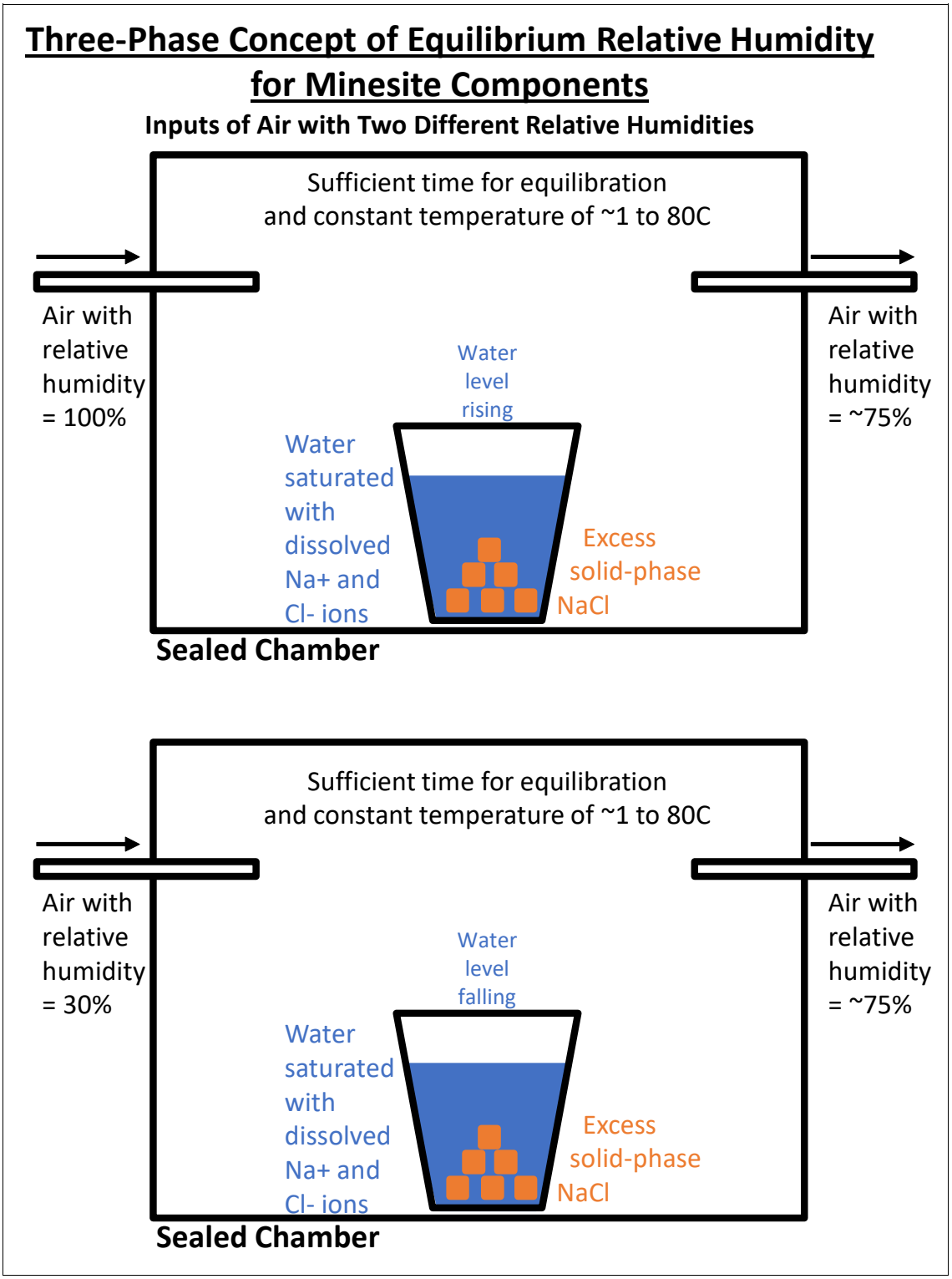

Figure 3-3. The simplified concept of Equilibrium Relative Humidity (ERH) for a salt solution with excess solid salt that can lower the relative humidity (RH) of high-RH air, or raise the RH of low-RH air, to a stable value.

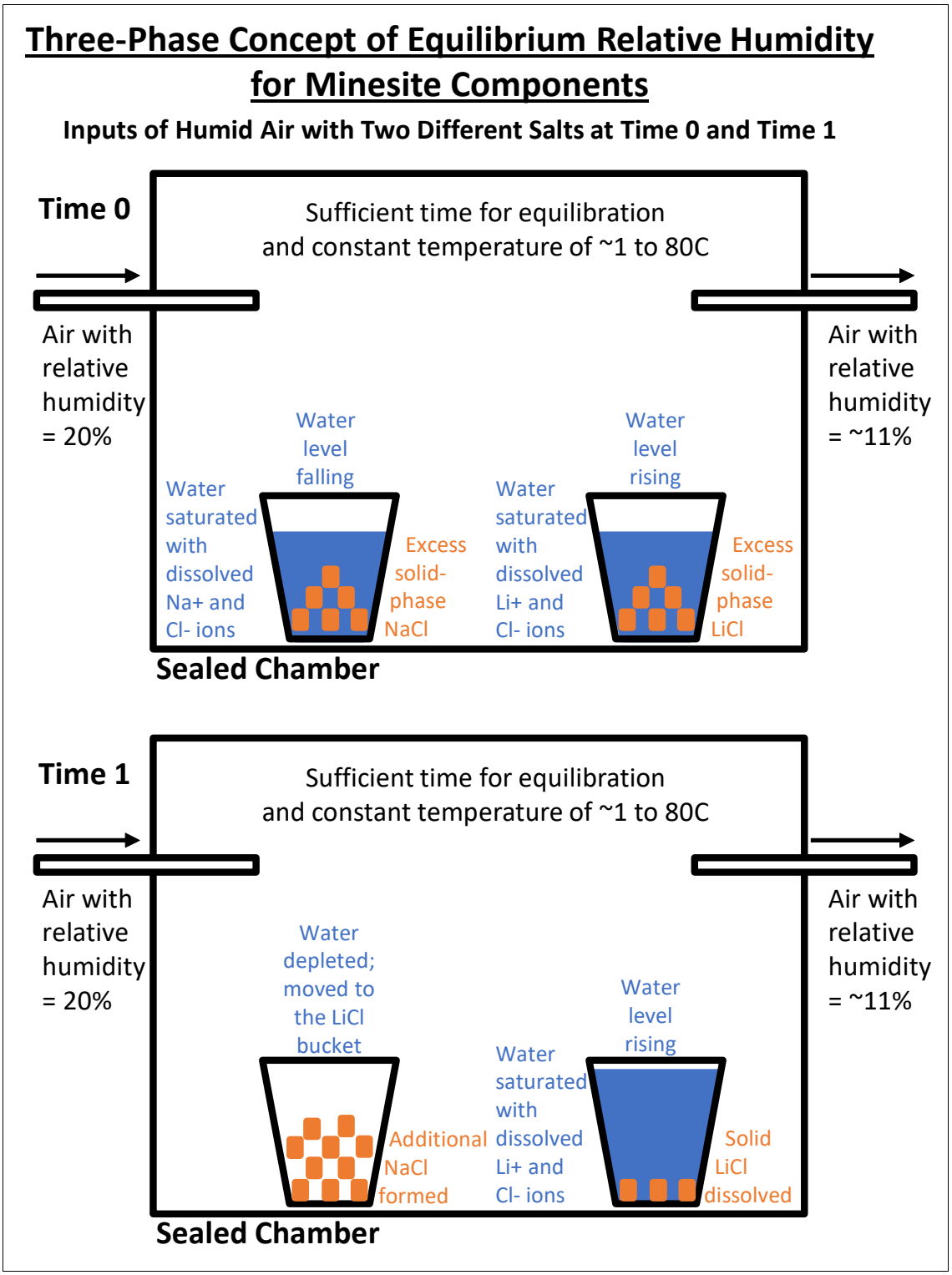

Figure 3-4. The simplified concept of Equilibrium Relative Humidity (ERH) for two different salt solutions with excess solid salts, with differing ERH values, leading to a net change in RH and to a redistribution of water through time.

- These relatively simple scenarios do not include complexities like (1) strong dynamics of the gas and/or aqueous phases, (2) natural aqueous solutions containing dozens of dissolved elements, or (3) kinetics of RH changes, which are discussed below.

- The temperature dependence of ERH between approximately 1 and 90°C is typically relatively minor (Figure 3-2), in spite of the large variation in corresponding absolute humidity with increasing temperature (Figure 2-1). This is because the activity of water (Equations 3-1 and 3-3) directly controls the relative humidity and only indirectly the absolute humidity depending on the temperature. Note that evaporation and condensation of water involve significant amounts of heat transfer, and this could affect the local temperature which in turn could affect RH and AH. These feedback processes lead to "complex three-phase effects" (Sections 3.2 and 7).

- Freshly exposed primary mineral surfaces like pyrite (Equation 2-5) react if there is sufficient H_2O as water or vapour (AH). Once reacted, aqueous concentrations in the water film increase and/or soluble secondary minerals form. This can lead to the ERH mechanism becoming operative, maintaining vapour and water levels so that primary minerals like pyrite can continue to react.

3.2 A Full-Scale Example Involving Soluble Minerals from Published Literature in the 1970's

An interesting written exchange took place in the 1970's in the Journal of Sedimentary Petrology (Kinsman, 1976; Walton, 1978) on whether the relative humidity or the interplay of absolute humidity and temperature was more important for the formation of sequential marine evaporite facies (precipitated salts) responding to humidity. This issue also applies to Figure 3-4.

Kinsman (1976) focussed on a relatively simple scenario of sabkhas (brine pools of isolated, evaporating ocean water) with stagnant overlying air containing various relative humidities. If the RH remained at or above 76%, then only calcium-sulphate minerals (gypsum or anhydrite) would precipitate as solids due to their relative high Equilibrium Relative Humidity of 76-93% RH, and halite (NaCl) could never form. Halite would precipitate only when RH levels decreased from 76 to 67%, and then potash (KCl) would precipitate only when RH levels decreased below 67%. This is a variation on Figure 3-4 that is based only on NaCl and LiCl.

The observed water ponded on sabkhas on mornings was attributed to cooling of air at night, which raised RH and caused the NaCl brines and precipitated salts to absorb H_2O from the air. Then daylight heating again lowered the RH and the ponded water evaporated. This was also observed in evaporite deposits in the Atacama Desert of Chile (Noe Dobrea et al., 2020).

Kinsman (1976) was inaccurate by saying, "The air masses above oceanic surfaces have mean annual relative humidity values rather close to 100%", when they are typically around 65-80% (e.g., Geophysical Fluid Dynamics Laboratory, 2014; Figure 3 in Pfahl and Sodemann, 2014). However, this does not invalidate Kinsman's general scenario, because the RH < 100% is due to many static and dynamic factors not considered.

Kinsman (1976) briefly addressed the flux of energy (heat) as being generally ignored in his paper and recognized that it potentially invalidated some general conclusions.

> "The energy relationships at first sight seem rather complex and do not appear readily resolvable with presently available data."

In response, Walton (1978) considered heat flux in more detail, envisioning dynamic scenarios where overlying air is moving and continuously replaced by wind (see also Stull, 2017). By evaluating absolute humidity and temperature separately, rather than combined as relative humidity, Walton illustrated how air movement and differences in temperature between air and brine (1) could anomalously cause evaporation of NaCl brine at RH above 76% and (2) could anomalously cause condensation into the NaCl brine at RH below 76%. This contradicts the simpler, stagnant scenario of Kinsman (1976) based on ERH. Walton explains,

> "My example implies that where temperature, absolute humidity and other factors are right, halite can precipitate despite high initial RH of air blowing across brine pools . . . At night, cooler breezes, with lower absolute humidity would be warmed by the brine and possibly even be able to evaporate water . . . "

Thus, ERH is a simplified concept based on generally static conditions or on minor dynamic conditions such as similar temperatures between air and water. These conditions can be expected in many minesite components, but exceptions are known. Dynamics conditions, and spatial and temporal energy fluxes, can invalidate simplistic ERH-based predictions in some cases (Harbeck, 1955). For example, the decrease in RH below a mineral's ERH initiates evaporation of the liquid water, which cools the solution and decreases the chemical activity of the water, which in turn changes the RH in the overlying air (e.g., Figure 2-1 above). There are also effects on the kinetic rate of evaporation. These positive and negative feedback loops are summarized graphically at the end of this Case Study (Figure 7-1).

Oroud (2019) emphasized the complexities that can invalidate the ERH concept under non-isothermal and dynamic conditions:

> "... brine activity is a transcendental composite function of water balance components, geochemical composition, thermodynamic feedbacks, and numerous atmospheric forcings."

Oroud provides several equations to illustrate these complexities far beyond those of Walton (1978).

4. Relative Humidity (RH) and Relatively Insoluble Minerals

4.1 Concepts and Explanations

The preceding Section 3 discussed how relatively soluble minerals can dissolve and lower water activity and, in turn, lower relatively humidity (RH). RH continues to decrease as the mineral dissolves until the solution is saturated and in equilibrium with that mineral, creating the ERH in the air phase (e.g., Figures 3-1 to 3-4).

However, Equation 3-3 shows that relatively insoluble minerals will have ERH values closer to 100%. Therefore, in this situation, complexities like Figures 3-3 and 3-4 will play a major role only when some soluble minerals are combined with the insoluble minerals (discussed in Section 4.2) either due to (1) their original occurrence and exposure in a minesite component or (2) water films becoming brines as they accumulate concentrations of ions like sodium and chloride.

Unlike soluble minerals, relatively insoluble minerals can be envisioned as having "hard" persistent surfaces. As explained in Section 1 above, these surfaces will be coated with water films. Several researchers have studied these water films on relatively insoluble minerals, such as hematite and gibbsite, which have been found inside minesite components.

Boily et al. (2015) examined water films a few monolayers thick on various crystal faces of hematite (α-Fe_2O_3) from 0 to 19 Torr of water-vapour pressure at 25°C (0 to 85% RH). Based on classical molecular dynamics, their Figure 1 (adapted here as Figure 4-1) divides the formation of water films onto crystalline hematite into:

- "adsorption" with binding of a single monolayer of H_2O directly onto the hematite crystal surface, and
- "condensation" with binding of additional water layers onto the already "adsorbed" hematite-bound water.

Boily et al. (2015) found hematite-surface single-layer "adsorption" of H_2O vapour was dominant primarily at lower humidities. There was little additional contribution above ~30% RH (Figure 4-1) as it approached the estimated single-layer maximum of 16 H_2O sites/nm^2,reportedly a value close to the surface density of oxygen atoms in the crystal.

In contrast, "condensation" of H_2O layers increased significantly and exceeded adsorption of the single, bound layer above ~70% RH (Figure 4-1). However, mineral particle edges, and by extension rough surfaces, can significantly affect the growth, size, and lateral extent of the water films at a particular RH value.

Similar observations as these for hematite were also noted for gibbsite ($Al(OH)_3$) by Yeşilbaş and Boily (2016) and Yalcin et al. (2020) (see Section 4.2 next). Thus, Figure 4-1 with an inflection point around 45% RH in the combined trend may be a generic model for several relatively insoluble minerals.

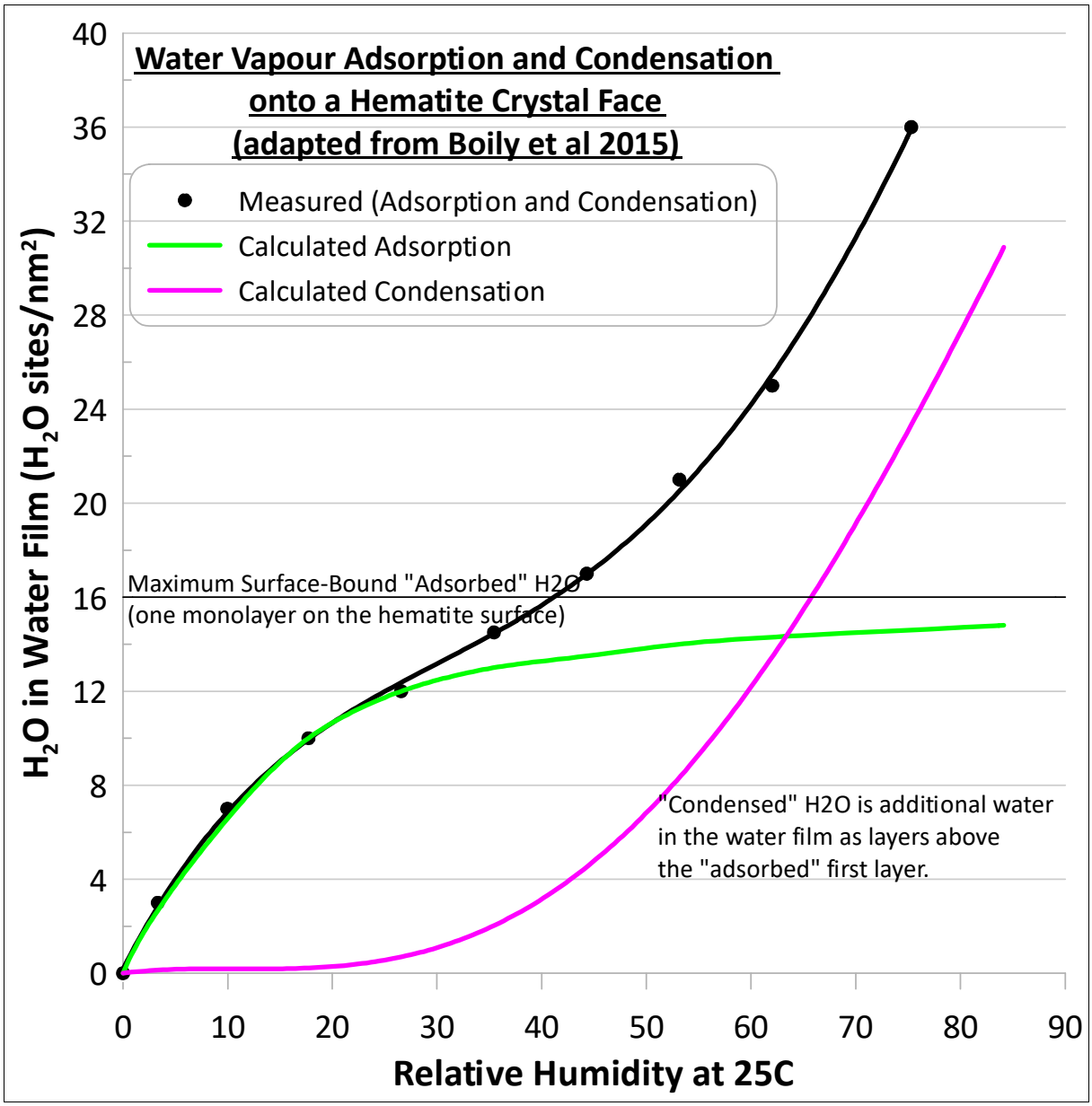

Figure 4-1. Formation of a water film on crystalline hematite with increasing relative humidity (RH) due to (1) adsorption of a single layer of H_2O bound to the hematite and (2) condensation of additional H_2O layers onto the adsorbed layer (adapted from Boily et al., 2015).

Interestingly, this view of water films as layers of H_2O bound to mineral surfaces conceptually conflicts with some other models like double-layer adsorption of ions to electrostatic surfaces (e.g., Figure 4-2) and like electrohydrodynamics (discussed further in Morin, 2020). To minimize this conflict, the binding of both H_2O and solvated aqueous ions to surfaces of a relatively insoluble mineral should be combined, but that is too ambitious for this Case Study.

4.2 Examples

Song and Boily (2013) examined the uptake of water and the formation of water films on relatively insoluble goethite (α-FeOOH) with varying additions of solid soluble NaCl, thus representing the complex scenario of mixed soluble and insoluble minerals or of insoluble minerals with concentrated water films (brines) on their surfaces. This work was done at 0% to 96% relative humidity at 25°C at pH ~ 7 and ~ 11.5. Their Figure 7 shows the trend with RH for only goethite resembles Figure 4-1 for hematite with an inflection point around 45% RH, whereas the trend with RH for only NaCl shows only a single curve concave upwards. Only mixtures of goethite with significant added NaCl substantially deviated from the goethite-only trend and only at RH above ~70%. This is consistent with the ERH of ~76% for NaCl above which humidity is adsorbed by the saturated NaCl solution (Figures 3-3 and 3-4).

Yeşilbaş and Boily (2016) examined and characterized water films for 21 relatively-insoluble-mineral water films in more detail at 25°C. Particle sizes less than 1 micrometer were coated with water films up to about five layers thick (see Figure 4-3, similar to Figure 4-1). In contrast, micrometer-sized mineral particles were coated with water films up to thousands of layers thick (Figure 4-4) at RH < 40% unlike finer particles (Figure 4-3). Thus, the single, directly "adsorbed" layer is not readily apparent or detected for these coarser particles. The reason for thick water films at RH < 40% on larger particles was not apparent, but various properties like surface roughness were suspected.

Steger (1982) experimentally tested the effect of relative humidity and temperature on the oxidation of pyrrhotite up to seven days duration. Steger's Figure 6 showed that the peak production rate of soluble ferrous iron and sulphate from pyrrhotite oxidation occurred between 57 and 59% RH at 50°C. Interpretations based on Figures 4-1 and 4-3 suggest this is the optimum thickness of water film for oxidizing pyrrhotite, where there is sufficient water film to allow and promote reactions but not too thick to slow reactions due to the increasing importance of mechanisms like diffusion. At 37% RH, sulfate formation occurred but oxide formation did not, possibly due to the relative lack of H_2O.

The repeated cycling of RH above and below ERH values of relatively soluble minerals (Section 3), and by extension of pairs of hydrated minerals (Section 5), with no added water can lead to flaking, slaking, and breaking of rocks like tuffs and sandstones (Sato and Hattanji, 2018). This is consistent with the findings of Jerz and Rimstidt (2003). In turn, this breakage can accelerate the chemical reactivity due to newly exposed minerals.

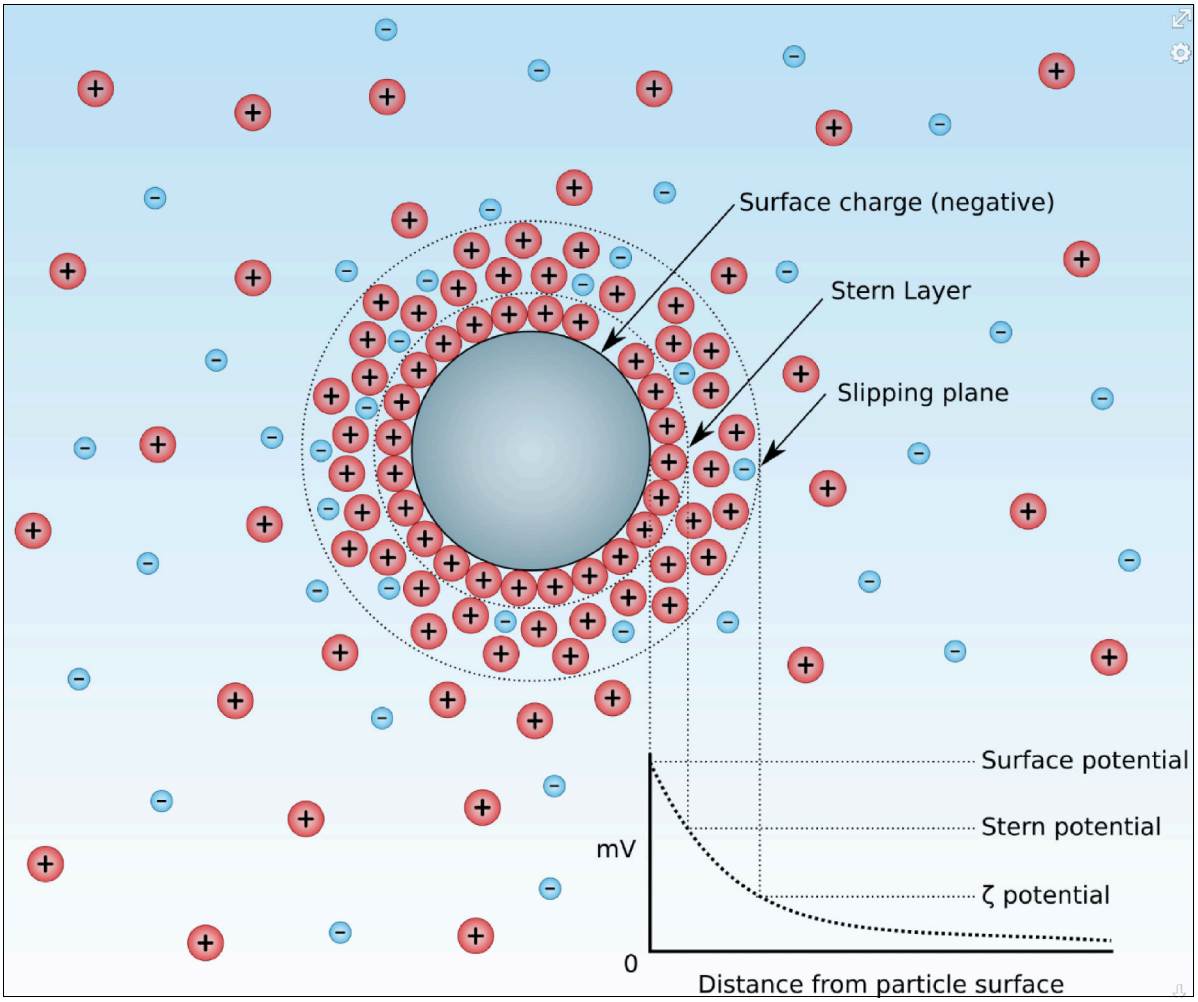

Figure 4-2. Schematic diagram of a negative particle-surface electrical charge and the associated strongly-adsorbed Stern Layer and the slipping plane caused by moving water that produces the zeta potential and streaming potential (from Wikipedia, 2002d and e).

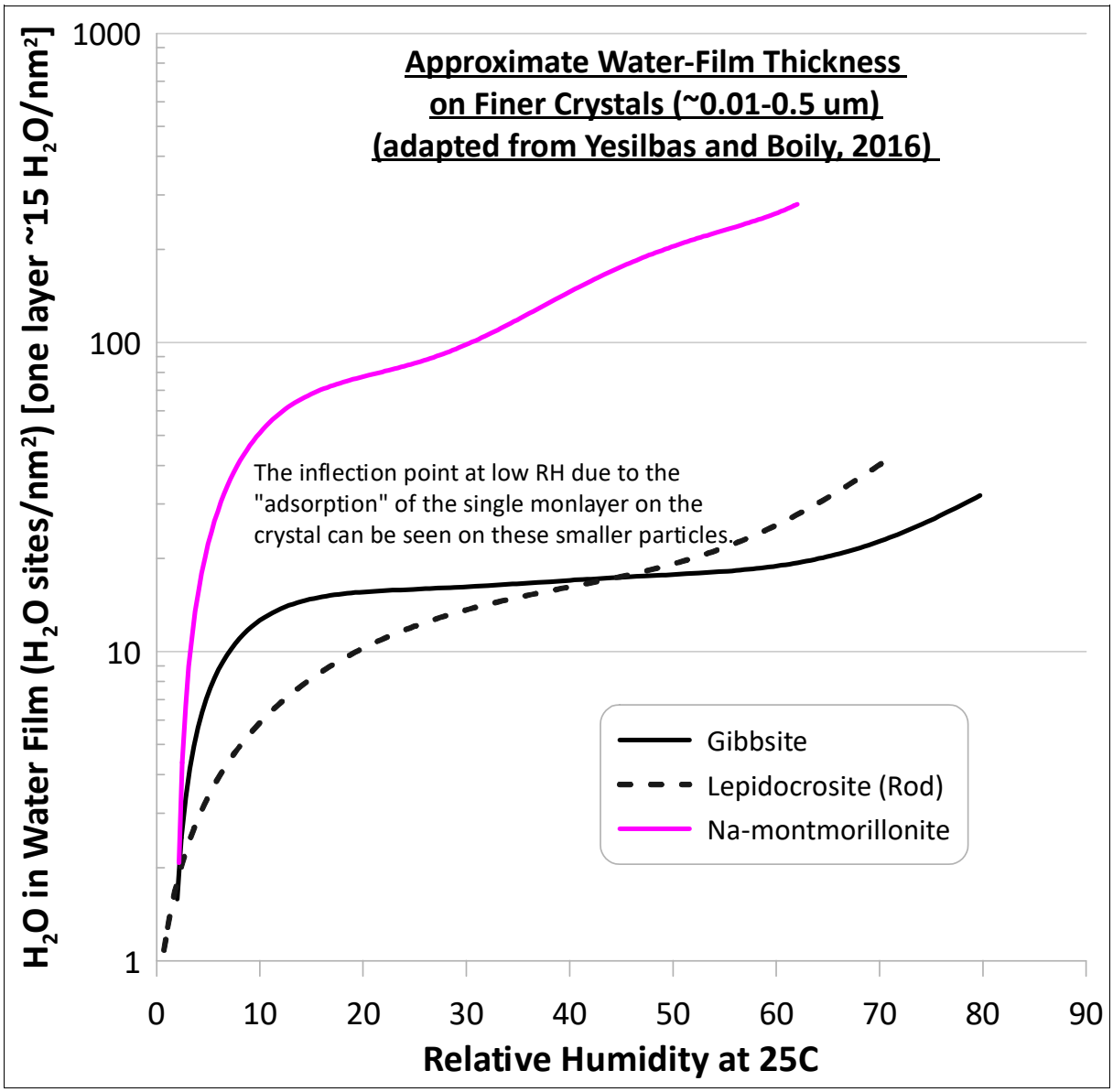

Figure 4-3. Water-film thickness vs. relative humidity on relatively finer crystals (~ < 1 um) of three minerals (adapted from Yeşilbaş and Boily, 2016).

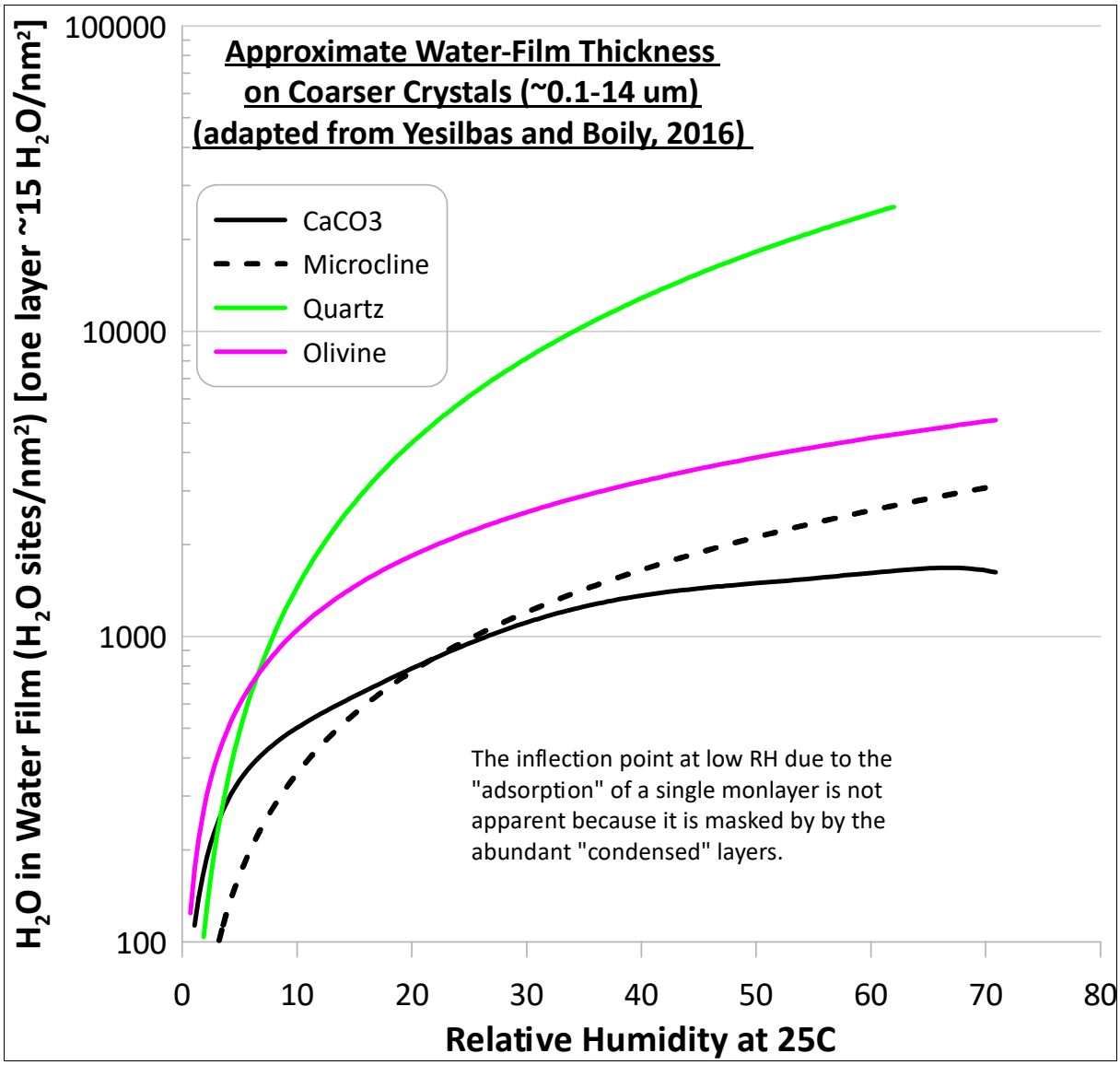

Figure 4-4. Water-film thickness vs. relative humidity on relatively coarser crystals (~ > 1 um) of four minerals (adapted from Ye ilba and Boily, 2016).

Dy et al. (2021) concluded that "consumption of oxygen by pyrite oxidation did not slow appreciably until the moisture content of the rock was around 0.6% wt. and the RH was 0.44". This experimental observation is consistent with Figures 4-1 and 4-3.

Consistent with the findings of the literature review in this Case Study, Dy et al. (2021) concluded,

> "Our measurements also show that waste rocks can effectively draw water from the pore-air space to drive the oxidation of pyrite. In a waste rock pile, it means that moisture can reach waste rocks through water vapour transport, to areas not influenced by seepage of liquid water. This implies that pore-air humidity may be sufficient for sustaining ARD-ML in mine waste dumps even without a fresh supply of meteoric or ground water. Since waste rocks can retain water in general, it is unlikely that rocks in commercial scale dumps can reach the level of dryness needed to stop sulfide oxidation completely."

5. Minerals with H_2O in Their Crystal Structures

5.1 General Concept

Many researchers have examined the effects of relative humidity (RH) on the hydration and dehydration of H_2O vapour into pairs of hydrated minerals with waters-of-crystallization, generally according to Equation 5-1.

$$MA{\bullet}aH_2O_{(solid)} + (b\text{-}a)H_2O_{(gas)} \leftrightarrow MA{\bullet}bH_2O_{(solid)} \quad \text{(Eq. 5-1)}$$

where M = one or more cations
A = one or more anions
a and b = constants representing various hydration states of a related pair of minerals

As a result, some mixtures of more-hydrated and less-hydrated versions of the same compound can be used as RH buffers (e.g., Chou et al., 2002), just like ERH values of mixed saturated water and relatively soluble minerals (Table 3-1 and Figure 3-2).

RH plays a major role in such hydration and dehydration in minerals due to its relationship to H_2O chemical activity, as it also does for relatively soluble minerals. Interestingly, much of the recently published work related to Equation 5-1 addresses conditions on Mars rather than on Earth.

5.2 Gypsum and Related Minerals

Gypsum (CaSO4•2H2O) is a common hydrated sulphate mineral in minesite components typically containing oxidizing sulphide minerals. The ERH for gypsum at 20°C in a saturated solution is reported at 98% RH (Winston and Bates, 1960).

Simplistically, gypsum is thought to dehydrate through bassanite (α and β $CaSO_4.0.5H_2O$) to anhydrite (primarily β $CaSO_4$ at lower temperatures), and then rehydrate in the opposite direction. Thermodynamically, the solubility of anhydrite falls below that of gypsum above ~42°C. Thus, anhydrite would be expected as the thermodynamically favoured mineral at higher temperatures above 42°C, although studies back to 1903 suggest the transition temperature may range from 40 to 66°C (Van Driessche et al., 2012 and 2017).

Reality is even more complex.

Azimi et al. (2007) found that gypsum was metastable above 40°C, with the addition of strong sulphuric acid (significantly lowering pH) lessening the metastability and thus gypsum converting to anhydrite above 40°C. Azimi and Papangelakis (2011) expanded this earlier work and studied the dehydration of gypsum into anhydrite at both low temperature (<100°C) and at high temperature. At low temperature, gypsum dehydration accelerated with increasing temperature, increasing strong acidity, the addition of anhydrite "seed" crystals, and increasing NaCl addition, whereas the addition of $NiSO_4$ interfered with the dehydration. The dehydration was direct to anhydrite with no formation

of bassanite, and at 80°C was nearly complete in 10 days with anhydrite seeding and in 2 days with NaCl-sulphuric-acid addition. Despite the theoretical temperature of 45-50°C for dehydration, gypsum remained metastable for at least 20 days at 90°C in the absence of anhydrite seeding.

Other intermediate hydrates and hydration-dehydration pathways for $CaSO_4$ have been reported. For example, dehydration of gypsum can lead initially to anhydrite which then partially back-hydrates to bassanite, and the hydration of anhydrite creates $CaSO_4 \bullet 0.67H_2O$ with an ERH apparently around 50% (Tang et al., 2019).

Van Driessche et al. (2012) found that gypsum formed through the initial formation of nano-scale bassanite below its predicted solubility, followed by transformation into gypsum. Bassanite itself can contain H_2O ranging in proportion from 0.5 to 0.625 (Wikipedia, 2021f) and even up to 0.8 (Van Driessche et al., 2017).

At 23°C, bassanite hydrates to gypsum at RH of 73%, gypsum will absorb enough water from the atmosphere to dissolve (deliquesce) at RH of 92%, and smectite clays can exchange H_2O with hydrated sulphate minerals like gypsum within hours (Wilson and Bish, 2011; Torrance and Darvell, 1990).

Also, the biological activity of microorganisms can dehydrate gypsum (Huang et al. 2020).

As seen above in this subsection, there are contradictions and ambiguities in the low-temperature relationships among gypsum, bassanite, and anhydrite. Van Driessche et al. (2017) explained,

> "Although significant advances have been made in our understanding of the precipitation of solid phases in the $CaSO_4$–H_2O system, there is still a considerable dearth of basic information that is crucial for a complete and comprehensive model of nucleation, growth, and transformation of the different $CaSO_4$ phases."

5.3 Other Hydrated Minerals Relevant to Minesite Components

Chou and Seal (2003 and 2005) and Chou et al. (2002 and 2013) summarized the RH and temperature (T) relationships for several hydrated metal-sulphate groups (e.g., Cu, Mg, Zn, Fe^{2+}, Fe^{3+}, and Ni) sometimes found in minesite drainages. Notably, most of these minerals groups would not be found together at most minesites, and additional hydrates can occur. These hydration-dehydration reactions can lead to mass transport of chemical elements in the resulting vapour (Bortnikova et al. 2019).

The RH-T trends based on Equation 5-1 showed that many hydration-dehydration reactions took place in the RH range mostly between 40% and 80% at an ambient temperature of 20°C (Figure 5-1). Some exceptions included $CdSO_4$ and $CdSO_4 \bullet H_2O$ with an RH of 2.7% RH at 20°C (Young, 1967). Thus these reactions could buffer RH at these levels, similar to ERH for saturated solutions with excess relatively soluble minerals (Table 3-1 and Figure 3-2).

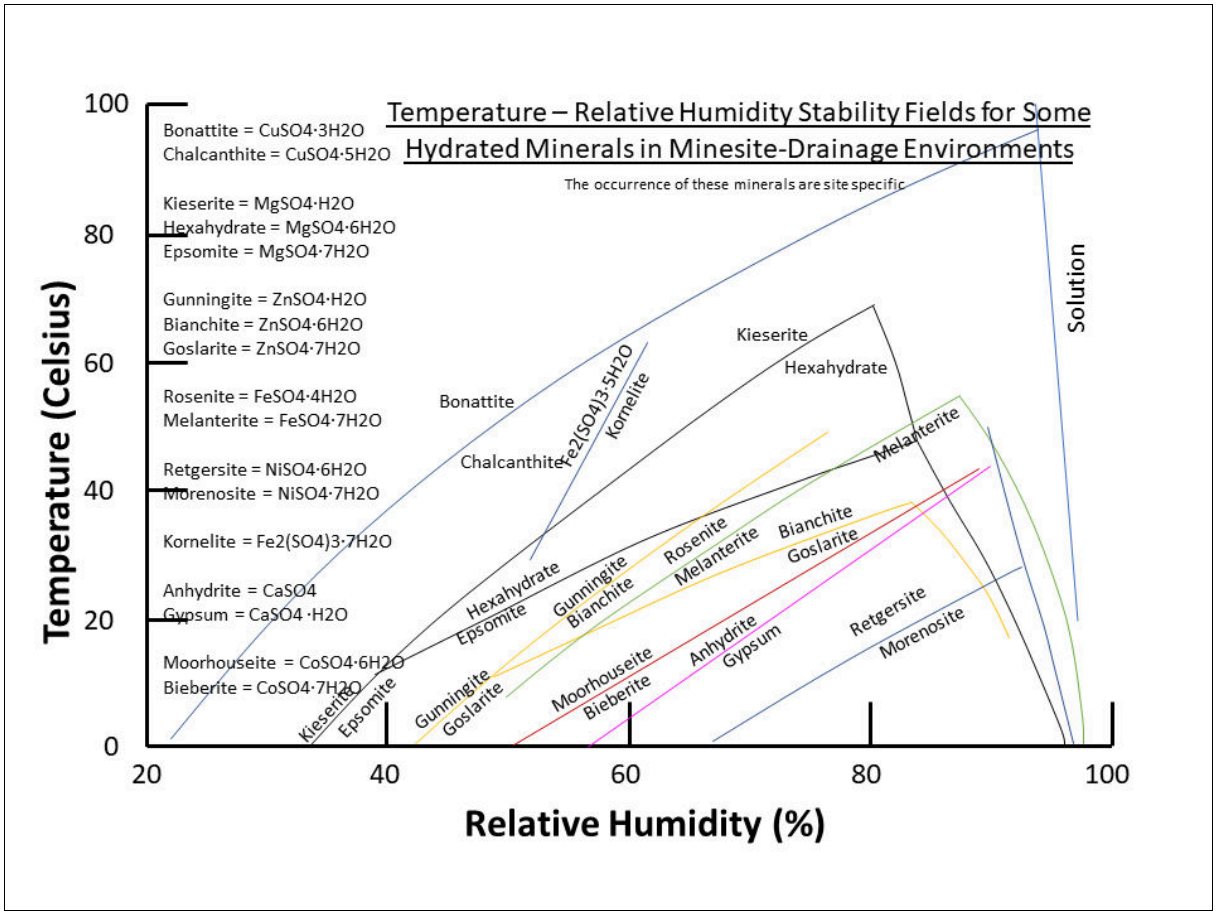

Figure 5-1. Compiled relative humidity and temperature relationships for several hydrated metal-sulphate groups found in some minesite components (adapted from Chou and Seal, 2003 and 2005, and Chou et al., 2002 and 2013); note: other hydrates are known within some of these groups and not all these groups typically occur together.

These hydration-dehydration-buffered RH values of Figure 5-1 at least partly overlap with soluble-mineral ERH values (Table 3-1) and with RH values for optimum physical and chemical thickness of water films (e.g., Figures 4-1 and 4-3, and Section 4.2). Thus, there are complex interactions and feedback loops among the H2O phases and even among various groups of minerals (Section 7).

Figure 5-1 also highlights a major potential error in many geochemical studies of minesite solid-phase samples where samples are dried at high temperatures such as above 100°C. Upon heating and drying, the sample would migrate towards the upper left of Figure 5-1. Thus, the results of such studies, like subsequent mineralogical examinations and kinetic testing, could be based on altered mineralogy that does not necessarily exist at same lower, ambient temperatures and RH levels at a minesite. This also likely often explains the reported presence of complex unit-cell minerals like schwertmannite at minesites.

Bonnell and Burridge (1935), Schumb (1923) and Wang et al. (2017) looked at other RH hydration-dehydration values, like for $ZnSO_4 \bullet 6H_2O$ to $ZnSO_4 \bullet 5H_2O$, $Na_2SO_4 \bullet 10H_2O$ to Na_2SO_4, and $BaCl_2 \bullet 2H2O$ to $BaCl2 \bullet H_2O$. Dozens of others, plus some amorphous phases (Schumb, 1923), likely exist.

Even then, hydrated minerals and pairs of minerals can evolve with time. For example, Xu and Parise (2012) showed some of the true complexity with some hydrated ferrous iron-sulphate minerals (Figure 5-2).

Jerz and Rimstidt (2003) and Jerz (2002) provided a more complete list of hydrated iron-sulphate minerals and measured equilibrated RH values for naturally-mixed-mineral samples dominated by one iron mineral:

- RH 80% for copiapite-rich ($Fe^{2+}Fe_4^{3+}(SO_4)_6(OH)_2 \bullet 20H_2O$) samples,
- RH 82% for melanterite-rich ($Fe^{2+}SO_4 \bullet 7H_2O$) samples,
- RH 88% for fibroferrite-rich ($Fe^{3+}(SO_4)(OH) \bullet 5H_2O$) samples, and
- RH 90% for halotrichite-rich ($Fe^{2+}Al_2(SO_4)_4 \bullet 22H_2O$) samples.

Dissolution of these and related minerals created acidic solutions and released other elements since other minerals were also present.

Peterson et al. (2007) reported the new hydrated mineral, Meridianiite ($MgSO_4 \bullet 11H_2O$), found in British Columbia and stable only at temperatures less than +2°C. Above +2°C, it dehydrates to epsomite ($MgSO_4 \bullet 7H_2O$) and water.

Sögütoglu et al. (2019) examined the hydration of $CuCl_2$ to $CuCl_2 \bullet 2H_2O$, K_2CO_3 to $K_2CO_3 \bullet 1.5H_2O$, $MgCl_2$ to $MgCl_2 \bullet 6H_2O$, and LiCl to $LiCl \bullet H_2O$ (with the latter hydration not included in simplified Figure 3-4), mostly from the perspective of heat storage and release. They found the hydration required a water film to occur, sometimes under metastable conditions, with the mobility of the water film increasing with increasing RH.

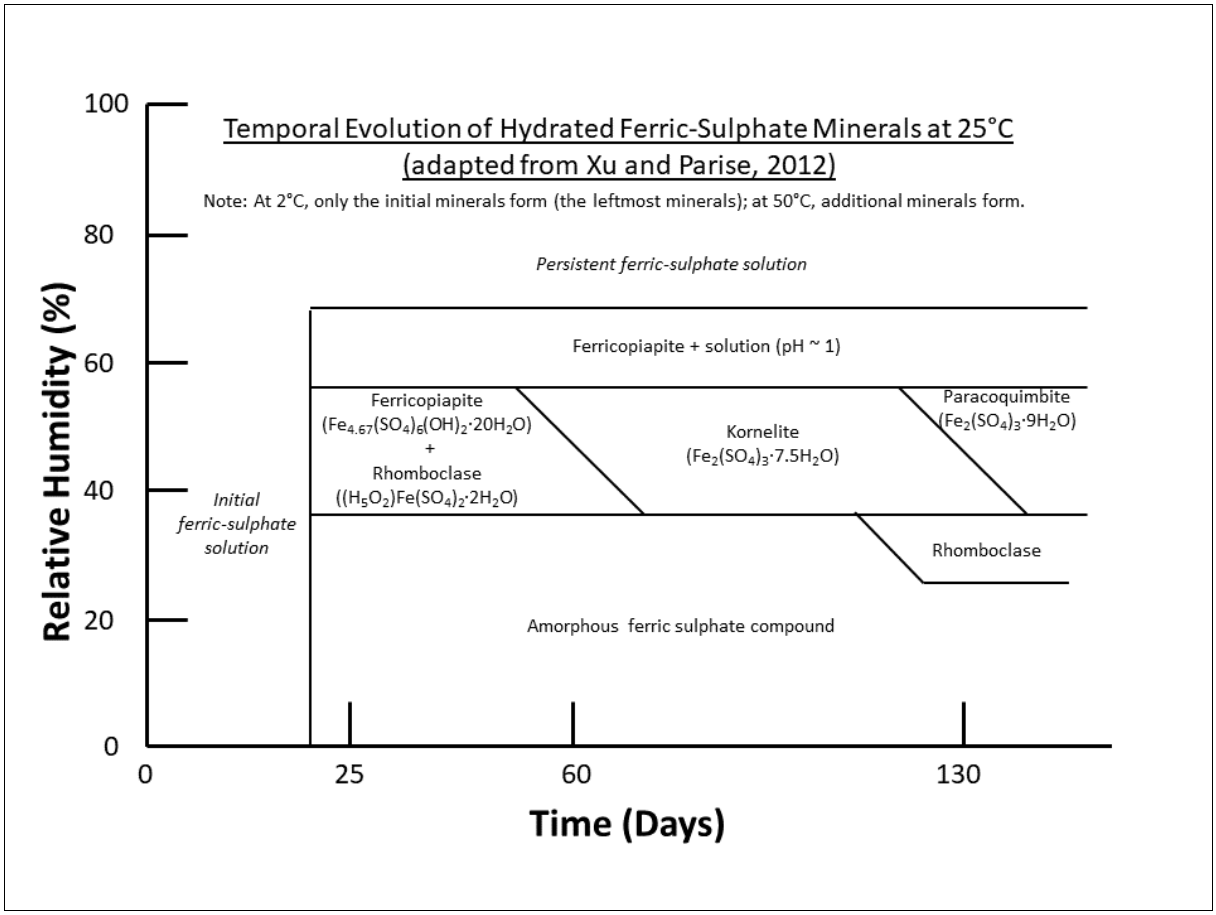

Figure 5-2. Relative-humidity-dependent temporal evolution of hydrated ferric-sulphate minerals at 25°C, showing some of the complexity in mineral hydration-dehydration reactions (adapted from Xu and Parise, 2012).

At approximately 30 to 50°C, the kinetics of dehydration were found to be relatively fast, mostly complete within many minutes to several hours, but showing complex trends with time, temperature, and pressure (Wheeler and Frost, 1955). At higher temperatures, hydration and dehydration are reversible within hours (Donkers et al., 2016).

In the end, no satisfactory explanations or predictive models, involving parameters like hydration number, ion size, and valence, have been found for equilibrated RH values of hydration-dehydration of variously hydrated minerals.

6. Mass Balance of H_2O among Phases

As shown in the previous sections, there are three phases of H_2O that can interact: vapour, liquid, and solid in hydrated minerals. This gives the impression that any one phase can have a significant effect on the other phases. In reality, the amount of H_2O in a phase can be orders of magnitude higher than the other phases, making it the dominant "reservoir" of, and primary control over, H_2O.

For this MDAG Case Study, the intention here is to obtain rough estimates of the number of moles of H_2O that might be found within minesite components in (1) the air phase in unsaturated pores, (2) the microscopic water films in unsaturated pores, (3) the water phase in saturated pores, and (4) the solid phase as the hydrated mineral, gypsum. As a supplement to (4), the amount of H_2O that would be consumed by pyrite based on Equation 2-5 is included.

Obviously, these results are highly specific to each minesite component, because they depend on many physical and geochemical properties. Therefore, some generalizations will be made here to obtain an approximate mass balance of H_2O (Table 6-1).

The resulting mass balance of H_2O (Table 6-2) shows that the liquid water phase contains at least an order of magnitude more H_2O than the other phases as long as more than 5% of the total pores contain water. Coming in second, as long as the wt-% of the reactive mineral is relatively low like 1 wt-%, the solid phase can contain or consume much less H_2O than in the water phase. Finally, coming in a distant third, the air phase in unsaturated pores would generally have the least amount of H_2O, but the relative amounts as vapour and as water film depend on the particle size.

Table 6-1. Generalizations and assumptions used here to obtain an approximate mass balance of H_2O in minesite components (see Table 6-2 for results and Appendix A for calculations)
A total volume of 1 m^3 within a minesite component
A temperature of 25°C
A porosity of 30% filled with 100% stagnant air at 100% RH or with 100% stagnant water
A specific gravity of the solid-phase of 2.7
Particle diameters of the solid phase of 1 cm and 0.1 mm
Water films on the particles, when the pores are not fully saturated, roughly four H_2O layers thick and thus about 1 nm
The solid phase containing 1 wt-% gypsum containing solid H_2O or 1 wt-% pyrite consuming H_2O according to Equation 2-5

Table 6-2. The mass balance of H_2O among stagnant phases in a generalized minesite component (based on Table 6-1 and Appendix A)	
H_2O Reservoir	H_2O Content in moles
Porespace, as 30% of Total Volume	
100% Air, Saturated with H_2O, Except for Microscopic Water Films	
Air	0.12
Water Film on 1 cm or 0.1 mm Particles	0.02 or 2.2
100% Water	
Water	16,600
Solid Phase, as 70% of Total Volume	
Containing 1 wt-% gypsum	220
H_2O consumed by 1 wt-% pyrite	550

7. Conclusion

This MDAG Case Study 71 has reviewed many dozens of publications and re-interpreted some of that information. The main objective was to understand better the interactions between various phases of H_2O relevant to minesite components and to other open environmental systems containing combinations of minerals. These H_2O phases, as they can occur within minesite components, are: (gaseous) vapour expressed as humidity, liquid water particularly in microscopic water films, and solid H_2O in "hydrated" minerals.

The interactions and negative or positive feedback loops were found to be complex (Figure 7-1). These are not easily understood intuitively or modelled. For vapour, relative humidity (RH) was found to be more important for understanding the interactions than absolute humidity (AH). This is because RH is related to the linked H_2O chemical activities in the vapour and water.

To better understand the effects and interactions of RH on microscopic water films and mineral surfaces, it became important to separate minerals into the two endpoints of (1) relatively soluble minerals like some chlorides and (2) relatively insoluble minerals like feldspars and some oxides. Additionally, hydrated minerals play an important role somewhere between the two endpoints. When these mineral groups are combined, as can be found in minesite components, the interactions among RH and the other H_2O phases become more complex (Figure 7-2).

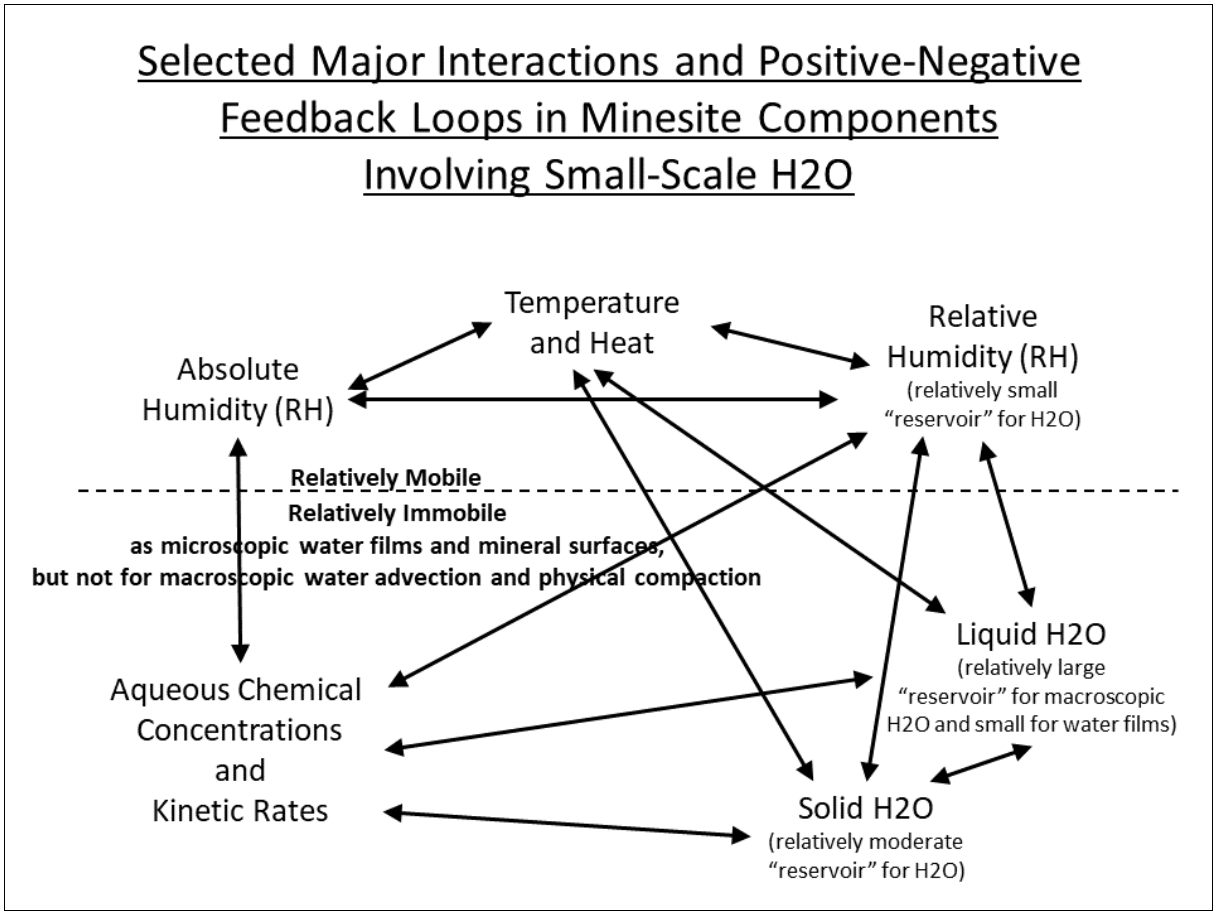

Figure 7-1. Summary of major interactions and feedback loops involving humidity and other H_2O phases on small scales in minesite components based on this review.

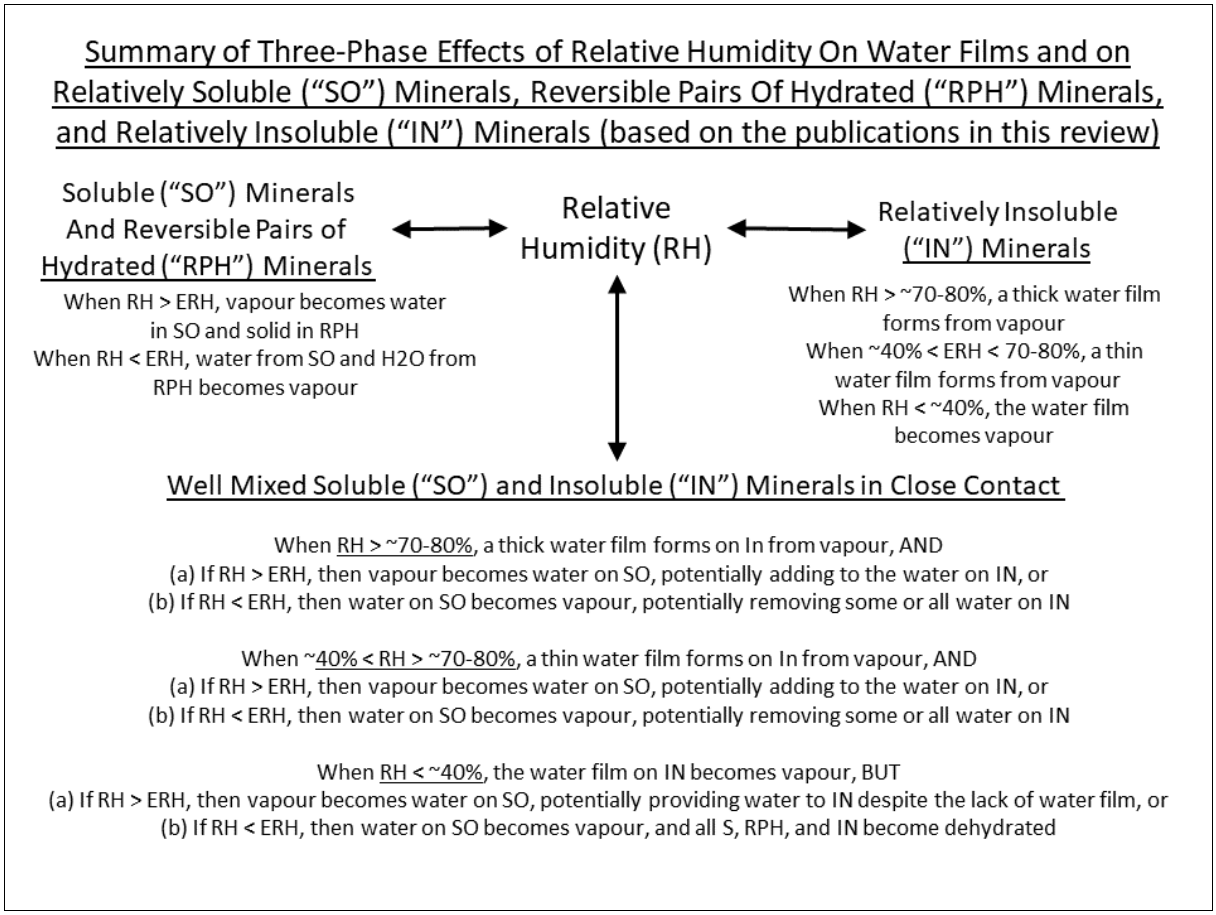

Figure 7-2. Summary of the three-phase effects of relative humidity on water and solids based on individual groups of minerals discussed here and a thorough mixture of all types.

8. References

Azimi, G., V.G. Papangelakis, and J.E. Dutrizac. 2007. Modelling of calcium sulphate solubility in concentrated multi-component sulphate solutions. Fluid Phase Equilibria, 260, p. 300-315. DOI: 10.1016/j.fluid.2007.07.069

Azimi, G., and V.G. Papangelakis. 2011. Mechanism and kinetics of gypsum-anhydrite transformation in aqueous electrolyte solutions. Hydrometallurgy, 108, p. 122-129. DOI: 10.1016/j.hydromet.2011.03.007

Boily, J-F., M. Yeşilbaş, M. Md. Uddin, L. Baiqing, Y. Trushkina, and G. Salazar-Alvarez. 2015. Thin water films at multifaceted hematite particle surfaces. Langmuir, 48, p. 13127-13137. DOI: 10.1021/acs.langmuir.5b03167

Bonnell, D.G.R., and L.W. Burridge. 1935. The dissociation pressures of some salt hydrates. Transactions of the Faraday Society, 31, p. 473-478. DOI: 10.1039/TF9353100473

Bortnikova, S., N. Abrosimova, N. Yurkevich, V. Zvereva, A. Devyatova, O. Gaskova, O. Saeva, T. Korneeva, O. Shuvaeva, N. Pal'chik, V. Chernukhin, and A. Reutsky. 2019. Gas transfer of metals during the destruction of efflorescent sulfates from the Belovo Plant Sulfide Slag, Russia. Minerals, 9, 344. DOI: 10.3390/min9060344

Bonanno, G., A.A. Carotenuto, L. Crovini, and M. Dell'Isola. 1994. A comparison of ideal and real moist air models for calculating humidity ratio and relative humidity in the 213.15 to 473.15 K range and up to a pressure of 1 MPa. International Journal of Thermophysics, 15, p. 483-504. DOI:

Carotenuto, A., and M. Dell'Isola. 1996. An experimental verification of saturated salt solution-based humidity fixed points. International Journal of Thermophysics, 17, p. 1423-1439. DOI: 10.1007/BF01438677

Chou, I-M, and R.R. Seal II. 2005. Acquisition and evaluation of thermodynamic data for bieberite-moorhouseite equilibria at 0.1 MPa. American Mineralogist, 90, p. 912-9178. DOI: 10.2138/am.2005.1695

Chou, I-M, and R.R. Seal II. 2003. Acquisition and evaluation of thermodynamic data for morenosite-retgersite equilibria at 0.1 MPa. American Mineralogist, 88, p. 1943-1948. DOI: 10.2138/am-2003-11-1237.

Chou, I-M., R.R. Seal II, and A. Wang. 2013. The stability of sulfate and hydrated sulfate minerals near ambient conditions and their significance in environmental and planetary sciences. Journal of Asian Earth Sciences, 62, p. 734-758. DOI: 10.1016/j.jseaes.2012.11.027

Chou, I-M, R.R. Seal II, and B.S. Hemingway. 2002. Determination of melanterite-rozenite and chalcanthite-bonattite equilibria by humidity measurements at 0.1 MPa. American Mineralogist, 87, p. 108-114. DOI: 10.2138/am-2002-0112

Donkers, P.A.J., L. Pel, and O.C.G. Adan. 2016. Experimental studies for the cyclability of salt hydrates for thermochemical heat storage. Journal of Energy Storage, 5, p. 25-32. DOI: 10.1016/j.est.2015.11.005

Dy, E., K. Tufa, E. Fisher, Z-S. Liu, K. Morin, M. O'Kane, T. O'Hearn, C. Huang, and W. Qu. 2121. The relationships between negative pore-water potential, water content, relative humidity and sulfide oxidation in waste rock - A case study. 14th IMWA Congress 2021, Newport, Wales, United Kingdom, 12-16 July 2021.

Flatt, R.J., and J.W. Bullard. 2011. Why alite stops hydrating below 80% relative humidity. Cement and Concrete Research, 41, p. 987-992. DOI: 10.1016/j.cemconres.2011.06.001.

Geophysical Fluid Dynamics Laboratory. 2014. 47. Relative humidity over the oceans. Accessed July 2021 at: https://www.gfdl.noaa.gov/blog_held/47-relative-humidity-over-the-oceans/

Greenspan, L. 1977. Humidity fixed points of binary saturated aqueous solutions. Journal of Research of the National Bureau of Standards - A. Physics and Chemistry, 81A, p. 89-96. DOI: 10.6028/jres.081A.011

Harbeck, Jr., G.E. 1955. The Effect of Salinity on Evaporation. Studies of Evaporation, U.S. Geological Survey Professional Paper 272-A, p. 1-6. DOI:10.3133/PP272A

Huang, W., E. Ertekin, T. Wang, L. Cruz, M. Dailey, J. DiRuggiero, and D. Kisailus. 2020. Mechanism of water extraction from gypsum rock by desert colonizing microorganisms. Proceedings of the National Academy of Sciences of the United States of America, 117 (2) 10681-10687. DOI: 10.1073/pnas.2001613117

Jerz, J.K. 2002. Geochemical Reactions in Unsaturated Mine Wastes. Ph.D. Dissertation, Virginia Polytechnic Institute and State University. Accessed July 2012 at: https://vtechworks.lib.vt.edu/handle/10919/27246

Jerz, J.K., and J.D. Rimstidt. 2004. Pyrite oxidation in moist air. Geochimica et Cosmochimica Acta, 68, p. 701-714. DOI: 10.1016/S0016-7037(03)00499-X

Jerz, J.K., and J.D. Rimstidt. 2003. Efflorescent iron sulfate minerals: Paragenesis, relative stability, and environmental impact. America Mineralogist, 88, p. 1919-1932. DOI: 10.2138/am-2003-11-1235

Kinsman, D.J.J. 1976. Evaporites: Relative humidity control of primary mineral facies. Journal of Sedimentary Petrology, 46, p. 273-279.

Ma, L., C. Huang, Z-S. Liu, K. Morin, M. Aziz and C. Meints. Submitted. Prediction of Acid Rock Drainage in waste rock piles. Part 2: Water flow patterns and leaching process.

Ma, L., C. Huang, Z-S. Liu, K.A. Morin, M. Aziz, and C. Meints. 2019. Prediction of Acid Rock Drainage and Metal Leaching in waste rock piles. Part 1: Water film model for geochemical reactions and application to a full-scale case study. Journal of Contaminant Hydrology, 220, p. 98-107.

Morin, K.A. 2021. Diffusion-dominated flux of poregases and aqueous ions in minesite components - commonly modelled but rarely applicable because realistic fluxes are much faster. MDAG Internet Case Study #67, www.mdag.com/case_studies.html

Morin, K.A. 2020. MDAG-com Case Study 63 - Planetary and large-scale processes affecting minesite-drainage flows and chemistries. MDAG Internet Case Study #63, www.mdag.com/case_studies.html

Noe Dobrea, E.Z., R.M.E. Williams, W.E. Dietrich, A.D. Howard, J.C. Cawley, and R.P. Irwin III. 2020. Mineralogy of a sulfate-rich "Inverted Channel" in the Atacama Desert, Chile: Clues to its formation and preservation. Accessed July 2021 at: https://arxiv.org/ftp/arxiv/papers/2002/2002.09950.pdf

O'Brien, F.E.M. 1948. The control of humidity by saturated salt solutions. Journal of Scientific Instruments, 25, p. 73-76. DOI: 10.1088/0950-7671/25/3/305

Olynyk, P., and A.R. Gordon. 1943. The vapor pressure of aqueous solutions of sodium chloride at 20, 25, and 30° for concentrations from 2 molal to saturation. Journal of the American Chemical Society, 65, p. 224–226. DOI: 10.1021/ja01242a023

Oroud, I.M. 2019. Evaporites: Relative humidity control of primary mineral facies revisited. Hydrological Processes, 33, p. 395-404. DOI: 10.1002/hyp.13334

Peterson, R.C., W. Nelson, B. Madu, and H.F. Shurvell. 2007. Meridianiite: A new mineral species observed on Earth and predicted to exist on Mars. American Mineralogist, 92, p. 1756-1759. DOI: 0.2138/am.2007.2668

Pfahl, S., and H. Sodermann. 2014. What controls deuterium excess in global precipitation? Climate of the Past, 10,

p. 771-781. DOI: 10.5194/cp-10-771-2014

Richardson, G.M., and R.S. Malthus. 1955. Salts for static control of humidity at relatively low levels. Journal of Applied Chemistry, 5, p. 557-567. DOI: 10.1002/jctb.5010051006

Robinson, R.A., and V.E. Bower. 1965a. An additivity rule for the vapor pressure lowering of aqueous solutions. Journal of Research of the National Bureau of Standards - A. Physics and Chemistry, 69A, p. 365-367. DOI: 10.6028/jres.069A.037

Robinson, R.A., and V.E. Bower. 1965b. Thermodynamics of the ternary system: Water-sodium-chloride-barium-chloride at 25°C. Journal of Research of the National Bureau of Standards - A. Physics and Chemistry, 69A, p. 19-27. DOI: 10.6028/jres.069A.004

Santos, S., and A. Verdaguer. 2016. Imaging water thin films in ambient conditions using atomic force microscopy. Materials, 9, 182. Doi: 10.3390/ma9030182

Sato, M., and T. Hattanji. 2018. A laboratory experiment on salt weathering by humidity change: salt damage induced by deliquescence and hydration. Progress in Earth and Planetary Science, 5:84. DOI: 10.1186/s40645-018-0241-2

Schumb, W.C. 1923. The dissociation pressures of certain salt hydrates by the gas-current saturation method. Journal of the American Chemical Society, 45, p. 342-354. DOI: 10.1021/ja01655a011

Sögütoglu, L-C., M. Steiger, J. Houben, D. Biemans, H.R. Fischer, P. Donkers, H. Huinink, and O.C.G. Adan. 2019. Understanding the hydration process of salts: The impact of a nucleation barrier. Crystal Growth and Design, 19, p. 2279-2288.

Song, X., and J-F. Boily. 2013. Water vapor adsorption on goethite. Environmental Science and Technology, 47, p. 7171-7177. DOI: 10.1021/es400147

Steger, H.F. 1982. Oxidation of sulphide minerals VII. Effect of temperature and relative humidity on the oxidation of pyrrhotite. Chemical Geology, 35, p. 281-295

Stull, R. 2017. Chapter 4 Water Vapor. IN: Practical Meteorology: An Algebra-Based Survey of Atmospheric Science, v. 1.02b. Accessed July 2021 at: https://www.eoas.ubc.ca/books/Practical_Meteorology/

Tang, Y., J. Gao, C. Liu, X. Chen, and Y. Zhao. 2019. Dehydration pathways of gypsum and the rehydration mechanism of soluble anhydrite γ-CaSO4. ACS Omega, 4, p. 7636-7642. DOI: 10.1021/acsomega.8b03476

Torrance, A., and B.W. Darvell. 1990. Effect of humidity on calcium sulphate hemihydrate. Australian Dental Journal, 35, p. 230-235. DOI: 10.1111/j.1834-7819.1990.tb05399.x

Van Driessche, A.E.S., T.M. Stawski, L.G. Benning, and M. Kellermeier. 2017. Calcium Sulfate Precipitation Throughout Its Phase Diagram. Chapter 12 in New Perspectives on Mineral Nucleation and Growth. Springer International Publishing. DOI: 10.1007/978-3-319-45669-0

Van Driessche, A.E.S., L.G. Benning, J.D. Rodriguez-Blanco, M. Ossorio, P. Bots, and J.M. Garcia-Ruiz. 2012. The role and implications of bassanite as a stable precursor phase to gypsum precipitation. Science, 336, p. 69-72. DOI: 10.1126/science.1215648

Walton, A.W. 1978. Evaporites: Relative humidity control of primary mineral facies: A discussion. Journal of Sedimentary Petrology, 48, p. 1357-1378.

Wang, Y., I-M. Chou, M. Zheng, and X. Hou. 2017. Acquisition and evaluation of thermodynamic data for

mirabilite-thenardite equilibria at 0.1 MPa. Journal of Chemical Thermodynamics, 111, p. 221-227. DOI: 10.1016/j.jct.2017.03.028

Wexler, A., and S. Hasegawa. 1954. Relative humidity-temperature relationships of some saturated salt solutions in the temperature range 0° to 50°C. Journal of Research of the National Bureau of Standards, 53, p. 19-26. DOI: 10.6028/jres.053.003

Wheeler, R.C., and G.B. Frost. 1955. A comparative study of the dehydration kinetics of several hydated salts. Canadian Journal of Chemistry, 33, p. 546-561. DOI: 10.1139/v55-064

Wilson, S.A., and D.L. Bish. 2011. Formation of gypsum and bassanite by cation exchange reactions in the absence of free-liquid H2O: Implications for Mars. Journal of Geophysical Research, 116, E09010. DOI: 10.1029/2011JE003853

Wikipedia. 2021a. Humidity. Accessed July 2021 at: https://en.wikipedia.org/wiki/Humidity

Wikipedia. 2021b. Water Activity. Accessed July 2021 at: https://en.wikipedia.org/wiki/Water_activity

Wikipedia. 2021c. Equilibrium moisture content. Accessed July 2021 at: https://en.wikipedia.org/wiki/Equilibrium_moisture_content

Wikipedia. 2020d. Zeta potential. Accessed July 2021 at: https://en.wikipedia.org/wiki/Zeta_potential

Wikipedia. 2021e. Double layer (surface science). Accessed July 2021 at: https://en.wikipedia.org/wiki/Double_layer_(surface_science)

Wikipedia. 2020f. Bassanite. Accessed July 2021 at: https://en.wikipedia.org/wiki/Bassanite

Winston, P.W., and D.H. Bates. 1960. Saturated solutions for the control of humidity in biological research. Ecology, 41, p. 232-237. DOI: 10.2307/1931961

Xu, W., and J.B. Parise. Temperature and humidity effects on ferric sulfate stability and phase transformation. American Mineralogist, 97, p. 378-383. DOI: 10.2138/am.2012.3927

Yalcin, S.E., B.A. Legg, M. Yeşilbaş, N.S. Malvankar, and J-F Boily. 2020. Direct observation of anisotropic growth of water films on minerals driven by defects and surface tension. Science Advances, 6, eaaz9807. DOI: 10.1126/sciadv.aaz9708

Yeşilbaş, M., and J-F. Boily. 2016. Particle size controls on water adsorption and condensation regimes at mineral surfaces. Scientific Reports, 6:32136. DOI: 10.1038/srep32136

Young, J.F. 1967. Humidity control in the laboratory using salt solutions - A review. Journal of Applied Chemistry, 17, p. 241-245. DOI: 10.1002/jctb.5010170901

Zhang, Y., X. Ouyang, and Z. Yang. 2019. Microstructure-Based Relative Humidity in Cementitious System Due to Self-Desiccation. Materials, 12, 1214. DOI: 10.3390/ma12081214.

APPENDIX A. Calculations of Values in Table 6-2 based on Values in Table 6-1

Total Volume = 1 m^3

Porosity = 0.30, so volume of pores = 0.3 m^3 and volume of solids = 0.7 m^3
Specific gravity = 2.7, so weight of solids = 1890 kg

Porespace

- 100% air at 100% saturation with H_2O vapour at 25°C contains 0.12 moles H_2O (0.4 moles H_2O from Figure 2-1 * porespace volume of 0.3 m^3)

Particle diameters of 0.1 mm (10^{-4} m) and 1 cm (10^{-2} m) have particle-surface areas of ~0.20 m^2/kg and 20 m^2/kg, respectively (from MDAG Grain 3.0), and thus total surface areas of 378 m^2 (0.20 m^2/kg * 1890 kg) and 37,800 m^2, respectively.

The approximate diameter of a molecule of H_2O is 0.25 nm. The thickness of a water film with four layers would be roughly 1 nm. Therefore, the volumes of these water films are about $3.8x10^{-5}$ m^3 H_2O and $3.8x10^{-7}$ m3 H_2O, respectively.

The density of water at 25°C is approximately 997 kg/m^3. Therefore, the weight and moles for the two particles sizes are 0.39 g H_2O or 0.02 moles H_2O, and 39 g H_2O or 2.2 moles H_2O, respectively.

- 100% water in 0.3 m^3 at 25°C contains 299,000 g H_2O (0.30 m^3 * 997,000 g/m^3) or 16,600 moles H_2O.

Solids

1 wt-% gypsum in the solid phase would weight 18,900 g (1890 kg * 0.01 * 1000). The atomic mass of gypsum is approximately 172 g/mol, so 1 wt-% gypsum is 110 moles of gypsum. One mole of gypsum contains two moles of H_2O. Therefore, 1 wt-% gypsum contains 220 moles H_2O.

1 wt-% pyrite in the solid phase would weigh 18,900 g. The atomic mass of pyrite is about 120 g/mol, so 1 wt-% pyrite is 158 moles of pyrite. According to Equation 2-5, one mole of pyrite consumes 3.5 moles of H_2O. Therefore, 1 wt-% pyrite consumes roughly 550 moles of H_2O.